Convex Optimization of Distributed Cooperative Detection in Multi-Receiver Molecular Communication

Yuting Fang, *Student Member, IEEE*, Adam Noel, *Member, IEEE*, Nan Yang, *Member, IEEE*, Andrew W. Eckford, *Senior Member, IEEE*, and Rodney A. Kennedy, *Fellow, IEEE*

Abstract—In this paper, the error performance achieved by cooperative detection among K distributed receivers in a diffusion-based molecular communication (MC) system is analyzed and optimized. In this system, the receivers first make local hard decisions on the transmitted symbol and then report these decisions to a fusion center (FC). The FC combines the local hard decisions to make a global decision using an N-out-of-K fusion rule. Two reporting scenarios, namely, perfect reporting and noisy reporting, are considered. Closed-form expressions are derived for the expected global error probability of the system for both reporting scenarios. New approximated expressions are also derived for the expected error probability. Convex constraints are then found to make the approximated expressions jointly convex with respect to the decision thresholds at the receivers and the FC. Based on such constraints, suboptimal convex optimization problems are formulated and solved to determine the optimal decision thresholds which minimize the expected error probability of the system. Numerical and simulation results reveal that the system error performance is greatly improved by combining the detection information of distributed receivers. They also reveal that the solutions to the formulated suboptimal convex optimization problems achieve near-optimal global error performance.

Index Terms—Molecular communication, multi-receiver cooperation, error performance, convex optimization.

I. INTRODUCTION

OVER the past decades there have been considerable advancements in the fields of nanotechnology and biological science, where the design and manufacturing of nanoscale ($< 0.1\mu$m) and microscale ($0.1 - 100\mu$m) devices, referred to as nanomachines, have begun to take shape [2]. Since nanomachines are only capable of performing simple computing, data storing, sensing, and actuation tasks, it is envisioned that they can be interconnected to execute more elaborate and challenging tasks in a collaborative and distributed manner. The resulting network, i.e., nanonetwork, is anticipated to expand the capabilities of single nanomachines by allowing them to exchange information and interact with each other. Looking 10–20 years ahead, nanonetworks will advance a diverse number of potential applications, such as disease detection, targeted drug delivery, and pollution control [3].

Molecular communication (MC) has been acknowledged as one of the most promising nanoscale communication paradigms in bio-inspired nanonetworks, due to its unique

potential benefits of bio-compatibility and low energy consumption [4]. In fact, MC is present in nature and used by biological entities and systems, such as molecules, cells, and microorganisms. In MC, a transmitter (TX) releases tiny particles such as molecules or lipid vesicles into a fluid medium, where the particles propagate until they arrive at a receiver (RX). The RX then detects the information encoded in these particles [5]. The simplest molecular propagation mechanism is free diffusion where the information-carrying particles propagate from the TX to the RX via Brownian motion. The TX does not need to expand any energy to use this mechanism.

One of the primary challenges posed by diffusion-based MC is that its reliability rapidly decreases when the TX-RX distance increases. One approach to enhancing its reliability is to use multiple RXs sharing common information to help transmission. In biological environments, some cells or organisms indeed share common information to achieve a specific task [6], e.g., calcium (Ca^{2+}) signaling [7]. In one process regulated by Ca^{2+} signaling, named excitation-contraction coupling, the cells in skeletal muscle share Ca^{2+} ions to induce the contraction of myofibrils [8].

The majority of the existing MC studies have focused on the modeling of a single-RX MC system. Recent studies, e.g., [9]–[16], have considered an MC system which consists of multiple RXs. For example, [9], [10] analyzed the transmission rate of a molecular broadcast system where a single TX communicates with multiple noncooperative RXs. In [11], simulations were performed to demonstrate the feasibility of a bio-nanosensor network where bacteria-based bio-nanomachines perform target detection and tracking. In [12], communication between two populations of bacteria through a diffusion channel was studied where each population acts as a TX or a RX. In [13], a microfluidic channel with two TX and RX pairs was explored. Focusing on the communication between a group of TXs and a group of RXs, [14] optimized the transmission rates that maximize the throughput and efficiency. A new stochastic model named reaction-diffusion master equation with exogenous input was proposed in [15] to characterize a MC system with multiple TXs and RXs. Recently, [16] designed a multiple-input multiple-output MC system and investigated the inter-symbol and inter-link interference therein, but did not consider cooperation between the links. While [9]–[16] stand on their own merits, these studies did not consider any active cooperation among multiple RXs. This indicates that the role of the cooperation among multiple RXs in determining the TX's intended symbol sequence in a multi-RX MC system has not been established in the literature.

We note that the cooperation among distributed detectors in wireless communications has been identified as an effective

means of improving performance. For example, cooperative spectrum sensing is achieved by allowing multiple secondary users to share sensing data to improve the detection quality of a primary user [17]. Generally, in a distributed detection system the data of the individual detectors is shared at a fusion center (FC). This data may be hard (binary) decisions, soft (multi-level) decisions, or quantized observations. The FC then appropriately combines the received data to yield a global inference [18] using a fusion rule, such as the AND rule and OR rule for hard decisions. In fact, logic operations and corresponding computations required at the FC, e.g., AND, OR, and addition operations, can be implemented at the molecular level [19], [20]. Therefore, MC is a suitable domain to apply distributed detection to improve transmission reliability. We note that this application has not been previously studied.

In this paper, we for the first time quantify and maximize the benefits of multi-RX cooperation in a cooperative diffusion-based MC system. Our goal is to establish a fundamental understanding of the reliability improvement brought by combining the detection results of distributed RXs at an FC. In our considered system, for each symbol transmitted from the TX, the RXs first independently make local hard decisions on the transmitted symbol and then report their decisions to the FC. We note that the role of the RXs in our considered system appears similar to that of decode-and-forward (DF) relays in wireless systems [21]. However, the results for DF relaying cannot be used in the MC system, due to the fact that the characteristics of the propagation channel and the methods for recovering the received symbols in MC systems are completely different from those in wireless systems. After receiving the local hard decisions, the FC fuses all decisions to make a global decision on the transmitted symbol using an N-out-of-K fusion rule. Here, we consider two different reporting scenarios from the RXs to the FC, namely, perfect reporting and noisy reporting. In this work, we assume that the FC does not feed back its global decision to RXs. We also assume that each RX transmits a unique type of molecule and the FC is able to simultaneously and independently detect the different types of molecules from the RXs[1] (as in [6]). We note that the use of a binary sequence is expected in molecular communications between nanomachines to exchange the amount of information required for executing complex collaborative tasks, such as disease detection and targeted drug delivery. Thus, in this work we consider the transmission of multiple binary symbols as a sequence and take the resultant inter-symbol interference (ISI) into account for the cooperative MC system.

To maximize the benefits of multi-RX cooperation in the system, we determine the jointly optimal decision thresholds at the RXs and FC such that the expected global error probability is minimized. We note that it is mathematically intractable to derive analytical expressions for such optimal thresholds. Therefore, we resort to convex optimization as an efficient and effective method to solve the joint optimization

problem. Since the expected global error probability is not necessarily convex with respect to thresholds at the RXs and FC, we conduct new convex analysis of the error performance for the system having a symmetric topology. Based on this analysis, we formulate convex optimization problems and find the solution via an efficient convex optimization algorithm. We note that finding the optimal thresholds at the RXs and FC via exhaustive search is time-consuming and requires relatively high complexity, compared with the adopted convex optimization. In the symmetric topology, the distances between the TX and the RXs are identical and the distances between the RXs and the FC are also identical. This results in independent and *identically* distributed observations at the RXs. We clarify that the assumption of the symmetric topology is to improve the tractability of our convex analysis and this assumption will be relaxed in future work. Also, for some practical applications, such as health monitoring, we may manually set the locations of the RXs and FC to ensure that the topology of the TX (e.g., monitored organism), the RXs (e.g., detectors), and the FC, is symmetric and reduce the complexity of system design and performance optimization. Also, the assumption of a symmetric topology is reasonable if the difference in distance between different $TX - RX - FC$ links is negligible, compared to the distance between the TX and the RXs. We note that the expected error probability of a point-to-point MC link is minimized in [22], by deriving a closed-form analytical expression for the optimal decision threshold at the RX. However, the derived optimal decision threshold in [22] cannot be applied or extended to the cooperative MC system.

The primary contributions of this paper, especially relative to our previous work [1], are summarized as follows:

1) We derive closed-form expressions for the expected global error probabilities of the cooperative MC system in the perfect and noisy reporting scenarios. We clarify that a symbol-by-symbol detection with a constant decision threshold at all RXs and the FC is considered in this derivation.

2) We derive new approximated expressions for the expected global error probability of the cooperative MC system in both reporting scenarios. We also derive additional convex constraints under which the approximated expressions are jointly convex with respect to the decision thresholds at the RXs and the FC.

3) Based on the derived convex approximations and constraints, we formulate suboptimal convex optimization problems for a given transmitted symbol sequence. For the sake of practicality, we then extend the formulated convex optimization problems such that a single optimal threshold is determined to minimize the average error performance over all realizations of transmitted symbol sequences.

Using numerical and simulation results, we demonstrate that the error performance of the cooperative MC system is much better than that of the point-to-point MC link. We also demonstrate the effectiveness of our formulated suboptimal convex optimization problems by showing that near-optimal global error performance is achieved by using the solutions

---

[1] We note that releasing a unique type of molecule at each RX may not be realistic in some cases. However, this assumption gives a lower bound on the error performance of the cooperative MC system using a hard decision fusion rule.
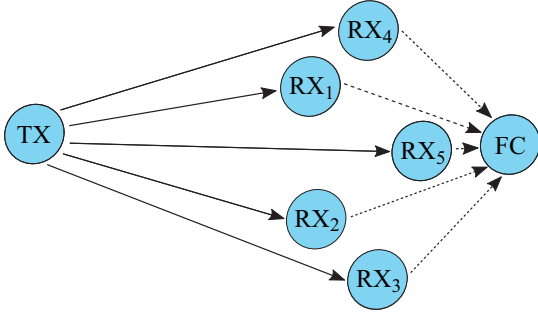
Fig. 1. An example of a cooperative MC system with $K = 5$, where the transmission from the TX to the RXs is represented by solid arrows and the decision reporting from the RXs to the FC is represented by dashed arrows.

to our formulated problems, i.e., the optimal thresholds. In this work, the optimality of the performance refers to the accuracy of the optimization to find the optimal thresholds in the symbol-by-symbol detection.

The rest of this paper is organized as follows. In Section II, we describe the system model. In Section III, we present the error performance analysis of the cooperative-RX MC system. In Section IV, we formulate convex optimization problems of the cooperative-RX MC system. Numerical and simulation results are provided in Section V. In Section VI, we conclude and describe future directions for this work.

II. SYSTEM MODEL

In this paper we consider a cooperative MC system in a three-dimensional space, as depicted in Fig. 1, which consists of one TX, a "cluster" of K RXs, and one device acting as an FC. The FC is not included in the set of RXs. We assume that the RXs are generally closer to the FC than to the TX to ensure reliable reporting channels from the RXs to the FC. We assume that all RXs and the FC are spherical observers. Accordingly, we denote V_{RX_k} and r_{RX_k} as the volume and the radius of the kth RX, RX_k, respectively, where $k \in \{1, 2, \ldots, K\}$. We also denote V_{FC} and r_{FC} as the volume and the radius of the FC, respectively. We also assume that the RXs and the FC are independent passive observers such that molecules can diffuse through them without reacting[2]. We further assume that all individual observations are independent of each other. In addition, we assume that the RXs operate in the half-duplex mode such that they do not receive information and report their local decisions at the same time.

In the considered system, the transmission of each information symbol from the TX to the FC via RXs is completed within three phases, detailed as follows:

- In the first phase, the TX transmits one symbol of information via type A_0 molecules to the RXs through the diffusive channel. The number of the released type A_0

---

[2]Although we cannot guarantee perfect independence between different RXs, the dependence between observations made at different RXs is extremely small. This is due to the fact that the time between adjacent samples at RXs is sufficiently long to ensure that observations at RXs are independent and each RX observes a small fraction of the total number of released molecules. Moreover, the validity of assuming independence will be demonstrated by the excellent agreement between analytical and simulation results depicted in Section V.

molecules is denoted by S_0. We assume that the diffusion of all individual molecules is independent. The type A_0 molecules transmitted by the TX are detected by all RXs. In this work we consider that the TX uses ON/OFF keying [24] to convey information. As per the rules of ON/OFF keying, the TX releases S_0 molecules of type A_0 to convey information symbol "1", and releases no molecules to convey information symbol "0". To enable ON/OFF keying, the information transmitted by the TX is represented by an L-length binary sequence where each element is "0" or "1". The sequence is denoted by $\mathbf{W}_{\mathrm{TX}} = \{W_{\mathrm{TX}}[1], W_{\mathrm{TX}}[2], \ldots, W_{\mathrm{TX}}[L]\}$, where $W_{\mathrm{TX}}[j]$, $j \in \{1, \ldots, L\}$, is the jth symbol transmitted by the TX. We assume that the probability of transmitting "1" in the jth symbol is P_1 and the probability of transmitting "0" in the jth symbol is $1 - P_1$, i.e., $\Pr(W_{\mathrm{TX}}[j] = 1) = P_1$ and $\Pr(W_{\mathrm{TX}}[j] = 0) = 1 - P_1$, where $\Pr(\cdot)$ denotes probability.

- In the second phase, each RX makes a local hard decision on the current transmitted symbol. We denote $\hat{W}_{\mathrm{RX}_k}[j]$ as the local hard decision on the jth transmitted symbol at RX_k. Then, the RXs simultaneously report their local jth hard decisions to the FC. We assume that RX_k transmits type A_k molecules, which can be detected by the FC. The number of the released type A_k molecules is denoted by S_k. We also assume that the channel between each RX and the FC is diffusion-based, and each RX uses ON/OFF keying to report its local hard decision.

- In the third phase, the FC obtains the decision at RX_k by receiving type A_k molecules over the $\mathrm{RX}_k - \mathrm{FC}$ link. We assume that the K $\mathrm{RX}_k - \mathrm{FC}$ links are independent. We denote $\hat{W}_{\mathrm{FC}_k}[j]$ as the received local decision of RX_k on the jth transmitted symbol at the FC. The FC combines all $\hat{W}_{\mathrm{FC}_k}[j]$ using an N-out-of-K fusion rule to make a global decision $\hat{W}_{\mathrm{FC}}[j]$ on the jth symbol transmitted by the TX, where N denotes the number of decisions of "1" received by the FC and K denotes the number of RXs. As per the N-out-of-K fusion rule, the FC declares a global decision of "1" when it receives at least N decisions of "1". There are several special cases of the N-out-of-K fusion rule, such as 1) majority rule where $N = \lceil K/2 \rceil$ and $\lceil x \rceil$ represents the smallest integer greater than or equal to x, 2) OR rule where $N = 1$, and 3) AND rule where $N = K$.

We define $\mathbf{W}_{\mathrm{TX}}^l = \{W_{\mathrm{TX}}[1], \ldots, W_{\mathrm{TX}}[l]\}$ as an l-length subsequence of the information transmitted by the TX, where $l \leq L$. We also define $\hat{\mathbf{W}}_{\mathrm{RX}_k}^l = \{\hat{W}_{\mathrm{RX}_k}[1], \ldots, \hat{W}_{\mathrm{RX}_k}[l]\}$ as an l-length subsequence of the local hard decisions at RX_k. We then define $\hat{\mathbf{W}}_{\mathrm{FC}_k}^l = \{\hat{W}_{\mathrm{FC}_k}[1], \ldots, \hat{W}_{\mathrm{FC}_k}[l]\}$ as an l-length subsequence of the received local decision of RX_k at the FC. We further define $\hat{\mathbf{W}}_{\mathrm{FC}}^l = \{\hat{W}_{\mathrm{FC}}[1], \ldots, \hat{W}_{\mathrm{FC}}[l]\}$ as an l-length subsequence of the global decisions at the FC.

We denote t_{trans} as the transmission interval time from the TX to the RXs and t_{report} as the report interval time from the RXs to the FC. Thus, the symbol interval time from the TX to the FC is given by $T = t_{\mathrm{trans}} + t_{\mathrm{report}}$. At the beginning of the jth symbol interval, i.e., $(j-1)T$, the TX transmits $W_{\mathrm{TX}}[j]$. After this the TX keeps silent until the start of the

$(j+1)$th symbol interval. We apply the weighted sum detector with equal weights [25] at the RXs and FC for detection. Thus, the RXs and FC each take multiple samples within their corresponding interval time, add the individual samples with equal weights, and compare the summation with a decision threshold. The decision thresholds at RX_k are denoted by ξ_{RX_k}. The decision thresholds at FC over the $RX_k - FC$ link denoted by ξ_{FC_k}. Here, the assumption of equal weights for all samples is adopted to limit the computational complexity of the detector and facilitate its usage in MC.

We now describe the sampling schedules of the RXs and FC. The FC or RX_k samples at a certain time t by counting the number of the molecules observed. All RXs sample at the same times[3] and take M_{RX} samples per symbol interval. The time of the mth sample for each RX in the jth symbol interval is given by $t_{RX}(j,m) = (j-1)T + m\Delta t_{RX}$, where Δt_{RX} is the time step between two successive samples at each RX, $m \in \{1, 2, \ldots, M_{RX}\}$, and $M_{RX}\Delta t_{RX} < t_{trans}$. At the time $(j-1)T + t_{trans}$, each RX reports its local decision for the jth interval via diffusion to the FC. We assume that the FC takes M_{FC} samples of *each* type of molecule in every reporting interval. The time of the $\tilde{m}$th sample of type A_k molecules at the FC in the jth symbol interval is given by $t_{FC}(j, \tilde{m}) = (j-1)T + t_{trans} + \tilde{m}\Delta t_{FC}$, where Δt_{FC} is the time step between two successive samples at the FC and $\tilde{m} \in \{1, 2, \ldots, M_{FC}\}$.

III. ERROR PERFORMANCE ANALYSIS

In this section, we analyze the expected global error probability[4] of the cooperative MC system. To this end, we denote $Q_{FC}[j]$ as the expected global error probability in the jth symbol interval for a *given* transmitter sequence $\mathbf{W}_{TX}^{j-1}$. Under the assumption that there is no *a priori* knowledge of $W_{TX}[j]$, we express $Q_{FC}[j]$ as

$$Q_{FC}[j] = P_1 Q_{md}[j] + (1 - P_1) Q_{fa}[j], \qquad (1)$$

where $Q_{md}[j]$ denotes the expected global missed detection probability (MDP) in the jth symbol interval and $Q_{fa}[j]$ denotes the expected global false alarm probability (FAP) in the jth symbol interval. By averaging $Q_{FC}[j]$ over all possible realizations of $\mathbf{W}_{TX}^{j-1}$ and across all symbol intervals, the expected average error probability of the cooperative MC system, $\overline{Q}_{FC}$, can be obtained. In the analysis, we address two different reporting scenarios, namely, perfect reporting and noisy reporting. In the perfect reporting scenario, we assume that no error occurs when RX_k reports to the FC, i.e., $\hat{W}_{FC_k}[j] = \hat{W}_{RX_k}[j]$. In the noisy reporting scenario, errors can occur when RX_k reports to the FC via diffusion[5].

---

[3]We note that all RXs may not be synchronized perfectly in some cases. Thus, we make the assumption of same sampling times of all RXs to explore the best error performance achieved by the cooperative MC system, which serves as a performance bound for practical systems. We also note that various methods can be adopted to achieve time synchronization among nanomachines, e.g., [26] and [27]. Therefore, the assumption of perfect synchronization is widely adopted in existing MC studies, e.g., [22], [25], and [16].

[4]All the expected error probabilities throughout this paper are derived for given $\mathbf{W}_{TX}^{j-1}$, unless otherwise specified.

[5]In this paper, the notations for the symbol interval time, the number of molecules for symbol "1" released by the TX, and the sampling schedules of the RXs in the perfect reporting scenario are the same as those in the noisy reporting scenario.

A. Perfect Reporting

In this subsection, we start our analysis by examining the error performance of the $TX - RX_k$ link. This examination is based on the analysis in [22]. We then use the results of this examination to analyze $Q_{md}[j]$ and $Q_{fa}[j]$ in the perfect reporting scenario to obtain $Q_{FC}[j]$.

1) $TX - RX_k$ Link: We first evaluate the probability of observing a given type A_0 molecule, emitted from the TX at $t = 0$, inside V_{RX_k} at time t, $P_{ob,0}^{(TX,RX_k)}(t)$. Given independent molecular behavior and assuming that the RXs are sufficiently far from the TX, we use [3, Eq. (1)] to write $P_{ob,0}^{(TX,RX_k)}(t)$ as

$$P_{ob,0}^{(TX,RX_k)}(t) = \frac{V_{RX_k}}{(4\pi D_0 t)^{3/2}} \exp\left(-\frac{d_{TX_k}^2}{4D_0 t}\right), \qquad (2)$$

where D_0 is the diffusion coefficient of type A_0 molecules in $\frac{m^2}{s}$ and d_{TX_k} is the distance between the TX and RX_k in m.

We denote $S_{ob,0}^{(TX,RX_k)}[j]$ as the sum of the number of molecules observed within V_{RX_k} in the jth symbol interval, due to the emission of molecules from the current and previous symbol intervals at the TX, $\mathbf{W}_{TX}^j$. As discussed in [22], $S_{ob,0}^{(TX,RX_k)}[j]$ can be accurately approximated by a Poisson random variable (RV) with the mean given by

$$\bar{S}_{ob,0}^{(TX,RX_k)}[j] = S_0 \sum_{i=1}^{j} W_{TX}[i]$$
$$\times \sum_{m=1}^{M_{RX}} P_{ob,0}^{(TX,RX_k)}\left((j-i)T + m\Delta t_{RX}\right). \qquad (3)$$

We also denote $U_{z,k}[j]$, $z \in \{0, 1\}$, as the conditional mean of $S_{ob,0}^{(TX,RX_k)}[j]$ when the most recent information symbol transmitted by the TX is $W_{TX}[j] = z$. Then, the decision at RX_k in the jth symbol interval is given by

$$\hat{W}_{RX_k}[j] = \begin{cases} 1, & \text{if } S_{ob,0}^{(TX,RX_k)}[j] \geq \xi_{RX_k}, \\ 0, & \text{otherwise.} \end{cases} \qquad (4)$$

Moreover, based on [22, Eq. (9)], the expected MDP of the $TX - RX_k$ link in the jth symbol interval for given $\mathbf{W}_{TX}^{j-1}$ is written as

$$P_{md,k}[j] = \Pr\left(S_{ob,0}^{(TX,RX_k)}[j] < \xi_{RX_k} \middle| W_{TX}[j] = 1, \mathbf{W}_{TX}^{j-1}\right), \qquad (5)$$

and the corresponding expected FAP is written as

$$P_{fa,k}[j] = \Pr\left(S_{ob,0}^{(TX,RX_k)}[j] \geq \xi_{RX_k} \middle| W_{TX}[j] = 0, \mathbf{W}_{TX}^{j-1}\right). \qquad (6)$$

Based on [23, Eq. 2.5], the cumulative distribution function (CDF) of $S_{ob,0}^{(TX,RX_k)}[j]$ is given by

$$\Pr\left(S_{ob,0}^{(TX,RX_k)}[j] < \xi_{RX_k} \middle| \mathbf{W}_{TX}^j\right) = \exp\left(-\bar{S}_{ob,0}^{(TX,RX_k)}[j]\right)$$
$$\times \sum_{\omega=0}^{\xi_{RX_k}-1} \frac{\bar{S}_{ob,0}^{(TX,RX_k)}[j]^\omega}{\omega!}. \qquad (7)$$

Using (7) and its complementary function, we can find the closed-form expressions for $P_{md,k}[j]$ and $P_{fa,k}[j]$.

2) Global Error Probability: We consider the cooperative MC system having a symmetric topology such that the RXs have independent and *identically* distributed observations. Under this consideration, we have $U_{z,k}[j] = U_z[j]$. Accordingly, we assume that the decision thresholds at the RXs are the same, i.e., $\xi_{\mathrm{RX}_k} = \xi_{\mathrm{RX}}$. Thus, we have $P_{\mathrm{md},k}[j] = P_{\mathrm{md}}[j]$ and $P_{\mathrm{fa},k}[j] = P_{\mathrm{fa}}[j]$.

We first consider the N-out-of-K fusion rule. Using [18, Eq. (3.4.30)] and [18, Eq. (3.4.31)] we evaluate $Q_{\mathrm{md}}[j]$ as

$$Q_{\mathrm{md}}[j] = 1 - \sum_{n=N}^{K} \binom{K}{n} (1 - P_{\mathrm{md}}[j])^n P_{\mathrm{md}}[j]^{K-n} \quad (8)$$

and evaluate $Q_{\mathrm{fa}}[j]$ as

$$Q_{\mathrm{fa}}[j] = \sum_{n=N}^{K} \binom{K}{n} P_{\mathrm{fa}}[j]^n (1 - P_{\mathrm{fa}}[j])^{K-n}. \quad (9)$$

For the OR rule, we obtain $Q_{\mathrm{md}}[j]$ and $Q_{\mathrm{fa}}[j]$ by substituting $N = 1$ into (8) and (9), leading to

$$Q_{\mathrm{md}}[j] = P_{\mathrm{md}}[j]^K \quad (10)$$

and

$$Q_{\mathrm{fa}}[j] = 1 - (1 - P_{\mathrm{fa}}[j])^K, \quad (11)$$

respectively. For the AND rule, we obtain $Q_{\mathrm{md}}[j]$ and $Q_{\mathrm{fa}}[j]$ by substituting $N = K$ into (8) and (9), resulting in

$$Q_{\mathrm{md}}[j] = 1 - (1 - P_{\mathrm{md}}[j])^K \quad (12)$$

and

$$Q_{\mathrm{fa}}[j] = P_{\mathrm{fa}}[j]^K, \quad (13)$$

respectively.

We note that the single-RX MC system, which consists of one TX, one RX, and one FC, is a special case of the cooperative MC system. Therefore, the expected error probability of the single-RX MC system in the jth symbol interval for a *given* transmitter sequence $\mathbf{W}_{\mathrm{TX}}^{j-1}$ in the perfect reporting scenario, $P_{\mathrm{e},1}[j]$, can be obtained by setting $K = 1$ in (8) and (9). Accordingly, the expected average error probability of the single-RX MC system, $\overline{P}_{\mathrm{e},1}$, can be obtained by averaging $P_{\mathrm{e},1}[j]$ over all possible realizations of $\mathbf{W}_{\mathrm{TX}}^{j-1}$ and across all symbol intervals.

B. Noisy Reporting

In this subsection, we first examine the error performance of the $\mathrm{TX} - \mathrm{RX}_k - \mathrm{FC}$ link, based on the analysis in [22], [28]. We then use the results of this examination to analyze $Q_{\mathrm{md}}[j]$ and $Q_{\mathrm{fa}}[j]$ in the noisy reporting scenario, enabling us to obtain $Q_{\mathrm{FC}}[j]$.

1) $\mathrm{TX} - \mathrm{RX}_k - \mathrm{FC}$ Link: We denote $P_{\mathrm{ob},k}^{(\mathrm{RX}_k,\mathrm{FC})}(t)$ as the probability of observing a given A_k molecule, emitted from the RX_k at $t = 0$, inside V_{FC} at time t. Due to the relatively close distance between the RXs and the FC, we find that (2)

or [3, Eq. (1)] cannot be used to evaluate $P_{\mathrm{ob},k}^{(\mathrm{RX}_k,\mathrm{FC})}(t)$. Thus, we resort to [28, Eq. (27)] to evaluate $P_{\mathrm{ob},k}^{(\mathrm{RX}_k,\mathrm{FC})}(t)$ as

$$P_{\mathrm{ob},k}^{(\mathrm{RX}_k,\mathrm{FC})}(t) = \frac{1}{2} \left[\mathrm{erf}\left(\tau_1\right) + \mathrm{erf}\left(\tau_2\right) \right]$$
$$- \frac{\sqrt{D_k t}}{d_{\mathrm{FC}_k}\sqrt{\pi}} \left[\exp\left(-\tau_1^2\right) - \exp\left(-\tau_2^2\right) \right], \quad (14)$$

where $\tau_1 = \frac{r_{\mathrm{FC}} + d_{\mathrm{FC}_k}}{2\sqrt{D_k t}}$, $\tau_2 = \frac{r_{\mathrm{FC}} - d_{\mathrm{FC}_k}}{2\sqrt{D_k t}}$, D_k is the diffusion coefficient of type A_k molecules in $\frac{\mathrm{m}^2}{\mathrm{s}}$, and d_{FC_k} is the distance between RX_k and the FC in m.

We denote $S_{\mathrm{ob},k}^{(\mathrm{RX}_k,\mathrm{FC})}[j]$ as the number of molecules observed within V_{FC} in the jth symbol interval, due to the emissions of molecules from the current and the previous symbol intervals at RX_k, $\hat{\mathbf{W}}_{\mathrm{RX}_k}^j$. We note that the TX and RX_k use the same modulation method and the $\mathrm{TX}-\mathrm{RX}_k$ and $\mathrm{RX}_k-\mathrm{FC}$ links are both diffusion-based. Therefore, $S_{\mathrm{ob},k}^{(\mathrm{RX}_k,\mathrm{FC})}[j]$ can be accurately approximated by a Poisson RV. We denote $\bar{S}_{\mathrm{ob},k}^{(\mathrm{RX}_k,\mathrm{FC})}[j]$ as the mean of $S_{\mathrm{ob},k}^{(\mathrm{RX}_k,\mathrm{FC})}[j]$ and obtain it by replacing S_0, $W_{\mathrm{TX}}[i]$, $P_{\mathrm{ob},0}^{(\mathrm{TX},\mathrm{RX}_k)}$, M_{RX}, m, and Δt_{RX} with S_k, $\hat{W}_{\mathrm{RX}_k}[i]$, $P_{\mathrm{ob},k}^{(\mathrm{RX}_k,\mathrm{FC})}$, M_{FC}, $\tilde{m}$, and Δt_{FC} in (3), respectively. We define $V_{\tilde{z},k}[j]$, $\tilde{z} \in \{0, 1\}$, as the conditional mean of $S_{\mathrm{ob},k}^{(\mathrm{RX}_k,\mathrm{FC})}[j]$ when the most recent information symbol transmitted by RX_k is $\hat{W}_{\mathrm{RX}_k}[j] = \tilde{z}$, given previous decisions at RX_k, $\hat{\mathbf{W}}_{\mathrm{RX}_k}^{j-1}$. Furthermore, we note that $\hat{W}_{\mathrm{FC}_k}[j]$ can be obtained by replacing $S_{\mathrm{ob},0}^{(\mathrm{TX},\mathrm{RX}_k)}[j]$ and ξ_{RX_k} with $S_{\mathrm{ob},k}^{(\mathrm{RX}_k,\mathrm{FC})}[j]$ and ξ_{FC_k} in (4), respectively. We now derive the expected MDP and FAP of the $\mathrm{TX} - \mathrm{RX}_k - \mathrm{FC}$ link in the jth symbol interval averaging over *all possible realizations* of $\hat{\mathbf{W}}_{\mathrm{RX}_k}^{j-1}$ for given $\mathbf{W}_{\mathrm{TX}}^{j-1}$, denoted by $\tilde{P}_{\mathrm{md},k}[j]$ and $\tilde{P}_{\mathrm{fa},k}[j]$, respectively. For a given $\mathbf{W}_{\mathrm{TX}}^{j-1}$, there are $2^{(j-1)}$ different possible realizations of $\hat{\mathbf{W}}_{\mathrm{RX}_k}^{j-1}$. We define $\mathcal{W}_j$ as the set containing all realizations of $\hat{\mathbf{W}}_{\mathrm{RX}_k}^{j-1}$. Considering all possible realizations of $\hat{\mathbf{W}}_{\mathrm{RX}_k}^{j-1}$ and their likelihood of occurrence, we first derive $\tilde{P}_{\mathrm{md},k}[j]$ and $\tilde{P}_{\mathrm{fa},k}[j]$ as

$$\tilde{P}_{\mathrm{md},k}[j] = \sum_{\hat{\mathbf{W}}_{\mathrm{RX}_k}^{j-1} \in \mathcal{W}_j} \left[\mathrm{Pr}\left(\hat{\mathbf{W}}_{\mathrm{RX}_k}^{j-1} \middle| \mathbf{W}_{\mathrm{TX}}^{j-1} \right) \right.$$
$$\times \left(\mathrm{Pr}\left(S_{\mathrm{ob},0}^{(\mathrm{TX},\mathrm{RX}_k)}[j] \geq \xi_{\mathrm{RX}} \middle| W_{\mathrm{TX}}[j] = 1, \mathbf{W}_{\mathrm{TX}}^{j-1} \right) \right.$$
$$\times \mathrm{Pr}\left(S_{\mathrm{ob},k}^{(\mathrm{RX}_k,\mathrm{FC})}[j] < \xi_{\mathrm{FC}_k} \middle| \hat{W}_{\mathrm{RX}_k}[j] = 1, \hat{\mathbf{W}}_{\mathrm{RX}_k}^{j-1} \right)$$
$$+ \mathrm{Pr}\left(S_{\mathrm{ob},0}^{(\mathrm{TX},\mathrm{RX}_k)}[j] < \xi_{\mathrm{RX}} \middle| W_{\mathrm{TX}}[j] = 1, \mathbf{W}_{\mathrm{TX}}^{j-1} \right)$$
$$\times \left. \left. \mathrm{Pr}\left(S_{\mathrm{ob},k}^{(\mathrm{RX}_k,\mathrm{FC})}[j] < \xi_{\mathrm{FC}_k} \middle| \hat{W}_{\mathrm{RX}_k}[j] = 0, \hat{\mathbf{W}}_{\mathrm{RX}_k}^{j-1} \right) \right) \right]$$
$$(15)$$

and

$$
\begin{aligned}
\tilde{P}_{\text{fa},k}[j] = \sum_{\hat{\mathbf{W}}_{\text{RX}_k}^{j-1} \in \mathcal{W}_j} & \Bigg[\Pr\left(\hat{\mathbf{W}}_{\text{RX}_k}^{j-1} \Big| \mathbf{W}_{\text{TX}}^{j-1} \right) \\
& \times \Bigg(\Pr\left(S_{\text{ob},0}^{(\text{TX},\text{RX}_k)}[j] \geq \xi_{\text{RX}} \Big| W_{\text{TX}}[j]=0, \mathbf{W}_{\text{TX}}^{j-1} \right) \\
& \times \Pr\left(S_{\text{ob},k}^{(\text{RX}_k,\text{FC})}[j] \geq \xi_{\text{FC}_k} \Big| \hat{W}_{\text{RX}_k}[j]=1, \hat{\mathbf{W}}_{\text{RX}_k}^{j-1} \right) \\
& + \Pr\left(S_{\text{ob},0}^{(\text{TX},\text{RX}_k)}[j] < \xi_{\text{RX}} \Big| W_{\text{TX}}[j]=0, \mathbf{W}_{\text{TX}}^{j-1} \right) \\
& \times \Pr\left(S_{\text{ob},k}^{(\text{RX}_k,\text{FC})}[j] \geq \xi_{\text{FC}_k} \Big| \hat{W}_{\text{RX}_k}[j]=0, \hat{\mathbf{W}}_{\text{RX}_k}^{j-1} \right) \Bigg) \Bigg],
\end{aligned}
\tag{16}
$$

respectively. Considering that the cooperative MC system having a symmetric topology, each RX_k has independent and identically distributed (i.i.d.) observations over each $\text{TX}-\text{RX}_k-\text{FC}$ link. Under this consideration, we have $V_{\tilde{z},k}[j] = V_{\tilde{z}}[j]$. Accordingly, we assume that the decision thresholds at the FC over RXs-FC links are the same, i.e., $\xi_{\text{FC}_k} = \xi_{\text{FC}}$. Thus, in (15) and (16), the likelihood of occurrence of each realization of $\hat{\mathbf{W}}_{\text{RX}_k}^{j-1}$ is the same for each RX_k. Also, the conditional MDP and FAP for the given realization is the same for each RX_k. This indicates that $\tilde{P}_{\text{md},k}[j]$ and $\tilde{P}_{\text{fa},k}[j]$ are the same for all RXs, i.e., $\tilde{P}_{\text{md},k}[j] = \tilde{P}_{\text{md}}[j]$ and $\tilde{P}_{\text{fa},k}[j] = \tilde{P}_{\text{fa}}[j]$. We note that the high complexity caused by considering $2^{(j-1)}$ possible realizations of $\hat{\mathbf{W}}_{\text{RX}_k}^{j-1}$ and their likelihood of occurrence make the evaluation of (15) and (16) cumbersome. To facilitate the calculation of (15) and (16), we consider only one possible realization of $\hat{\mathbf{W}}_{\text{RX}_k}^{j-1}$ and refer to this considered realization as the candidate. By only considering the candidate of $\hat{\mathbf{W}}_{\text{RX}_k}^{j-1}$, we then approximate (15) and (16) as

$$
\begin{aligned}
\tilde{P}_{\text{md}}[j] \approx & \Pr\left(S_{\text{ob},0}^{(\text{TX},\text{RX}_k)}[j] \geq \xi_{\text{RX}} \Big| W_{\text{TX}}[j]=1, \mathbf{W}_{\text{TX}}^{j-1} \right) \\
& \times \Pr\left(S_{\text{ob},k}^{(\text{RX}_k,\text{FC})}[j] < \xi_{\text{FC}} \Big| \hat{W}_{\text{RX}_k}[j]=1, \hat{\mathbf{W}}_{\text{RX}_k}^{j-1} \right) \\
& + \Pr\left(S_{\text{ob},0}^{(\text{TX},\text{RX}_k)}[j] < \xi_{\text{RX}} \Big| W_{\text{TX}}[j]=1, \mathbf{W}_{\text{TX}}^{j-1} \right) \\
& \times \Pr\left(S_{\text{ob},k}^{(\text{RX}_k,\text{FC})}[j] < \xi_{\text{FC}} \Big| \hat{W}_{\text{RX}_k}[j]=0, \hat{\mathbf{W}}_{\text{RX}_k}^{j-1} \right)
\end{aligned}
\tag{17}
$$

and

$$
\begin{aligned}
\tilde{P}_{\text{fa}}[j] \approx & \Pr\left(S_{\text{ob},0}^{(\text{TX},\text{RX}_k)}[j] \geq \xi_{\text{RX}} \Big| W_{\text{TX}}[j]=0, \mathbf{W}_{\text{TX}}^{j-1} \right) \\
& \times \Pr\left(S_{\text{ob},k}^{(\text{RX}_k,\text{FC})}[j] \geq \xi_{\text{FC}} \Big| \hat{W}_{\text{RX}_k}[j]=1, \hat{\mathbf{W}}_{\text{RX}_k}^{j-1} \right) \\
& + \Pr\left(S_{\text{ob},0}^{(\text{TX},\text{RX}_k)}[j] < \xi_{\text{RX}} \Big| W_{\text{TX}}[j]=0, \mathbf{W}_{\text{TX}}^{j-1} \right) \\
& \times \Pr\left(S_{\text{ob},k}^{(\text{RX}_k,\text{FC})}[j] \geq \xi_{\text{FC}} \Big| \hat{W}_{\text{RX}_k}[j]=0, \hat{\mathbf{W}}_{\text{RX}_k}^{j-1} \right),
\end{aligned}
\tag{18}
$$

where the candidate of $\hat{\mathbf{W}}_{\text{RX}_k}^{j-1}$ can be obtained using a biased coin toss method. Particularly, we model the ith decision at RX_k, $\hat{W}_{\text{RX}_k}[i]$, as $\hat{W}_{\text{RX}_k}[i] = |\lambda - W_{\text{TX}}[i]|$, where $i \in \{1, \cdots, j-1\}$ and $\lambda \in \{0, 1\}$ is the outcome of the coin toss with $\Pr(\lambda = 1) = P_{\text{md},k}[i]$ if $W_{\text{TX}}[i] = 1$ and $\Pr(\lambda = 1) = P_{\text{fa},k}[i]$ if $W_{\text{TX}}[i] = 0$. We assume that the candidate of $\hat{\mathbf{W}}_{\text{RX}_k}^{j-1}$ in (17) and (18) is the same at all RXs to ensure that $\tilde{P}_{\text{md},k}[j] = \tilde{P}_{\text{md}}[j]$ and $\tilde{P}_{\text{fa},k}[j] = \tilde{P}_{\text{fa}}[j]$ are still valid after adopting the approximations of $\tilde{P}_{\text{md}}[j]$ and $\tilde{P}_{\text{fa}}[j]$ in (17) and (18), respectively. We clarify that the candidate

is only considered for the *theoretical* evaluation of system error performance, i.e., the calculation of (17) and (18). We emphasize that we do not consider the same realizations of $\hat{\mathbf{W}}_{\text{RX}_k}^{j-1}$ at all RXs in our system model. Furthermore, in our simulations, each RX makes decisions independently and the realizations of $\hat{\mathbf{W}}_{\text{RX}_k}^{j-1}$ at all RXs are not necessarily identical. Our simulation results in Section V demonstrate the accuracy of (17) and (18).

In addition, the CDF of $S_{\text{ob},k}^{(\text{RX}_k,\text{FC})}[j]$ is obtained by replacing $S_{\text{ob},0}^{(\text{TX},\text{RX}_k)}[j]$, ξ_{RX_k}, $\mathbf{W}_{\text{TX}}^j$ and $\bar{S}_{\text{ob},0}^{(\text{TX},\text{RX}_k)}[j]$ with $S_{\text{ob},k}^{(\text{RX}_k,\text{FC})}[j]$, ξ_{FC}, $\mathbf{W}_{\text{RX}_k}^j$, $\bar{S}_{\text{ob},k}^{(\text{RX}_k,\text{FC})}[j]$ in (7), respectively. Using the CDFs of $S_{\text{ob},0}^{(\text{TX},\text{RX}_k)}[j]$ and $S_{\text{ob},k}^{(\text{RX}_k,\text{FC})}[j]$ and their complementary functions, we can find the closed-form expressions for $\tilde{P}_{\text{md},k}[j]$ and $\tilde{P}_{\text{fa},k}[j]$.

2) Global Error Probability: In the noisy reporting scenario, we obtain $Q_{\text{md}}[j]$ and $Q_{\text{fa}}[j]$ for the N-out-of-K rule, OR rule, and AND rule by replacing $P_{\text{md}}[j]$ and $P_{\text{fa}}[j]$ with $\tilde{P}_{\text{md}}[j]$ and $\tilde{P}_{\text{fa}}[j]$, respectively, in (8)–(13). We also note that the expected error probability of the single-RX MC system in the jth symbol interval for a *given* transmitter sequence $\mathbf{W}_{\text{TX}}^{j-1}$ in the noisy reporting scenario can be obtained by setting $K = 1$.

We note that the expected error probabilities of the cooperative MC system are also tractable if weighted sum detectors with different weights are considered at the RXs and FC for detection. Under this consideration, the mth sample at RX_k or FC in the jth symbol interval can be accurately approximated by a Poisson RV. Although the weighted sums of Poisson RVs, $S_{\text{ob},0}^{(\text{TX},\text{RX}_k)}[j]$ and $S_{\text{ob},k}^{(\text{RX}_k,\text{FC})}[j]$, are not Poisson RVs, the weighted sums of Gaussian approximations of the individual variables are Gaussian RVs. Thus, we can write the CDF of the Gaussian RVs and complementary functions to derive $P_{\text{md},k}[j]$, $P_{\text{fa},k}[j]$, $\tilde{P}_{\text{md},k}[j]$, and $\tilde{P}_{\text{fa},k}[j]$. Then we can derive the global error probabilities using (8)–(13) for the cooperative MC system in the perfect and noisy reporting scenarios.

IV. ERROR PERFORMANCE OPTIMIZATION

In this section, we present a novel analysis to determine the joint optimal ξ_{RX} and ξ_{FC} that minimize the global error probability of the cooperative MC system. To this end, we first derive the convex upper bounds on $Q_{\text{FC}}[j]$ for the OR rule, AND rule, and N-out-of-K rule[6] in the perfect and noisy reporting scenarios, allowing us to formulate the corresponding convex optimization problems for given $\mathbf{W}_{\text{TX}}^{j-1}$. We then extend the formulated convex optimization problems for given $\mathbf{W}_{\text{TX}}^{j-1}$ to the convex optimization problems for the *average* error performance over all possible realizations of $\mathbf{W}_{\text{TX}}^{j-1}$ and across all symbol intervals. This extension is due to two reasons. First, optimizing the instantaneous error performance for given $\mathbf{W}_{\text{TX}}^{j-1}$ may not be feasible in practice. This optimization mandates the precise knowledge of $\mathbf{W}_{\text{TX}}^{j-1}$ at RX_k, which cannot be realized in practice. Second, the repeated optimization of

---

[6]We clarify that the convex upper bounds for the OR rule, AND rule, and N-out-of-K rule are derived separately. This is due to the fact that the derived convex upper bounds for the N-out-of-K rule with $N = 1$ and $N = K$ are not as tight as those derived for the OR rule and AND rule, respectively.

the detection threshold for each realization of $\mathbf{W}_{\text{TX}}^{j-1}$ would demand a high computational overhead for RX_k.

A. Perfect Reporting

In this subsection, we formulate the convex optimization problems with respect to ξ_{RX} for the OR rule, AND rule, and N-out-of-K rule in the perfect reporting scenario. To achieve this, we first analyze the convexity of $P_{\text{md}}[j]^K$ and $P_{\text{fa}}[j]^K$ with respect to ξ_{RX}. Since $S_{\text{ob},0}^{(\text{TX,RX})}[j]$ is a Poisson RV with a discrete distribution, its convexity analysis with respect to ξ_{RX} is cumbersome. To overcome this cumbersomeness, we approximate the CDF of a Poisson RV X with mean λ by the CDF of a continuous Gaussian RV. We find that the accuracy of this approximation becomes higher when λ increases. Thus, the tightness of the approximation can be ensured by any method achieving large λ, such as increasing the number of molecules released, increasing the volume (radius) of RXs and FC, and choosing the optimal sampling period. Including a continuity correction, the CDF of the Gaussian RV is given by

$$\Pr(X < x) = \frac{1}{2}[1 + \Lambda(x, \lambda)], \qquad (19)$$

where $\Lambda(x, \lambda) = \text{erf}\left((x - 0.5 - \lambda)/\sqrt{2\lambda}\right)$. Applying (19) into (5) and (6), $P_{\text{md}}[j]$ and $P_{\text{md}}[j]$ are approximated as

$$P_{\text{md}}[j] \approx \frac{1}{2}[1 + \Lambda(\xi_{\text{RX}}, U_1[j])] \qquad (20)$$

and

$$P_{\text{fa}}[j] \approx 1 - \frac{1}{2}[1 + \Lambda(\xi_{\text{RX}}, U_0[j])], \qquad (21)$$

respectively. We now present the constraints making $P_{\text{md}}[j]^K$ and $P_{\text{fa}}[j]^K$ convex in the following theorem.

Theorem 1: $P_{\text{md}}[j]^K$ and $P_{\text{fa}}[j]^K$ are convex with respect to ξ_{RX}, if we impose the following convex constraints:

$$-0.5 - U_1[j] + \xi_{\text{RX}} \leq 0 \qquad (22)$$

and

$$0.5 + U_0[j] - \xi_{\text{RX}} \leq 0, \qquad (23)$$

respectively.

Proof: The convexity of $P_{\text{md}}[j]^K$ can be proven by showing that its second derivative with respect to ξ_{RX} is nonnegative [29]. We derive the second derivative of $P_{\text{md}}[j]^K$ as

$$\frac{\partial^2 P_{\text{md}}[j]^K}{\partial \xi_{\text{RX}}^2} = \frac{1}{2^K}\left(\frac{2(-1+K)K}{\pi}\Xi(-2+K, 2, 1)\right.$$
$$\left. + \sqrt{\frac{2}{\pi}}K(0.5 + U_1[j] - \xi_{\text{RX}})\Xi\left(-1+K, 1, \frac{3}{2}\right)\right), \quad (24)$$

where

$$\Xi(\alpha, \beta, \gamma) = \frac{(1 + \Lambda(\xi_{\text{RX}}, U_1[j]))^\alpha \Theta(\xi_{\text{RX}}, U_1[j])^\beta}{U_1[j]^\gamma} \qquad (25)$$

and $\Theta(x, \lambda) \triangleq \exp\left(-(0.5 + \lambda - x)^2/2\lambda\right)$. Due to the fact that the value of $\Lambda(x, \lambda)$ is between -1 and 1 and the value of $\Theta(x, \lambda)$ is always greater than zero, (24) is always

nonnegative if we impose the constraint (22). Following a similar procedure, we prove that $P_{\text{fa}}[j]^K$ is also convex with respect to ξ_{RX}, if we impose the constraint (23). ∎

We now analyze the convexity of $Q_{\text{fa}}[j]$ and $Q_{\text{md}}[j]$ for the three rules. For the OR rule, an upper bound on $Q_{\text{fa}}[j]$ is given by

$$Q_{\text{fa}}[j] \leq KP_{\text{fa}}[j], \qquad (26)$$

which is obtained by applying the first degree Taylor series approximation of $1 - (1 - P_{\text{fa}}[j])^K$ into (11) at $P_{\text{fa}}[j] = 0$. We find that this upper bound is tight when $P_{\text{fa}}[j]$ is small. We note that $P_{\text{fa}}[j]$ is convex with respect to ξ_{RX}, if we impose the constraint (23), which can be proven by considering $K = 1$ in Theorem 1. Thus, the upper bound in (26) is also convex with respect to ξ_{RX} under the same constraint, since it scales a convex function with a nonnegative constant. Also based on Theorem 1, $Q_{\text{md}}[j]$ for the OR rule, $P_{\text{md}}[j]^K$, is convex with respect to ξ_{RX}, if we impose the constraint (22). Therefore, the convex optimization problem for the cooperative MC system with the OR rule in the perfect reporting scenario is formulated as

$$\min_{\xi_{\text{RX}}} \quad P_1 P_{\text{md}}[j]^K + (1 - P_1) K P_{\text{fa}}[j]$$
$$\text{s.t.} \quad (22) \text{ and } (23). \qquad (27)$$

Due to the convexity of the objective function and the constraints, (27) can be quickly solved by efficient algorithms, e.g., the interior-point method [29]. Throughout this paper, we refer to the optimal threshold, i.e., the threshold in the feasible set that minimizes the objective function, as the solution to the convex optimization problem, where the feasible set is the set containing all of the thresholds that satisfy all constraints.

Next, we focus on the AND rule. Using a similar method as in (26), $Q_{\text{md}}[j]$ is upper-bounded by

$$Q_{\text{md}}[j] \leq KP_{\text{md}}[j]. \qquad (28)$$

We note that $P_{\text{md}}[j]$ is convex with respect to ξ_{RX} under the constraint (22), which can be proven by considering $K = 1$ in Theorem 1. Thus, (28) is also convex with respect to ξ_{RX} under the same constraint. Based on Theorem 1, $Q_{\text{fa}}[j]$ for the AND rule, $P_{\text{fa}}[j]^K$, is convex respect to ξ_{RX}, if we impose the constraint (23). Therefore, the convex optimization problem for the cooperative MC system with the AND rule in the perfect reporting scenario can be formulated as

$$\min_{\xi_{\text{RX}}} \quad P_1 K P_{\text{md}}[j] + (1 - P_1) P_{\text{fa}}[j]^K$$
$$\text{s.t.} \quad (22) \text{ and } (23). \qquad (29)$$

Finally, we consider the N-out-of-K rule. We rewrite (8) as

$$Q_{\text{md}}[j] = \sum_{\tilde{n}=K-N+1}^{K}\binom{K}{\tilde{n}}P_{\text{md}}[j]^{\tilde{n}}(1 - P_{\text{md}}[j])^{K-\tilde{n}}. \quad (30)$$

Based on (30) and (9), we verify that

$$Q_{\text{md}}[j] \leq \sum_{\tilde{n}=K-N+1}^{K}\binom{K}{\tilde{n}}P_{\text{md}}[j]^{\tilde{n}} \triangleq Q_{\text{md}}^+[j] \qquad (31)$$

and

$$Q_{\text{fa}}[j] \leq \sum_{n=N}^{K} \binom{K}{n} P_{\text{fa}}[j]^n \triangleq Q_{\text{fa}}^+[j]. \tag{32}$$

In Theorem 1, we showed that $P_{\text{md}}[j]^K$ and $P_{\text{fa}}[j]^K$ are convex with respect to ξ_{RX}, if we impose the convex constraints (22) and (23), respectively. We note that $P_{\text{md}}[j]^{\tilde{n}}$ and $P_{\text{fa}}[j]^n$, where $\tilde{n} \in \{K - N + 1, \ldots, K\}$ and $n \in \{N, \ldots, K\}$, are also convex with respect to ξ_{RX}, if we impose the convex constraints (22) and (23), respectively. The convexity of $P_{\text{md}}[j]^{\tilde{n}}$ and $P_{\text{fa}}[j]^n$ with respect to ξ_{RX} can be proven by replacing K with $\tilde{n}$ and n in the proof to Theorem 1, respectively. Since (31) and (32) are nonnegative weighted sums of convex functions, i.e., $P_{\text{md}}[j]^{\tilde{n}}$ and $P_{\text{fa}}[j]^n$, they are also convex with respect to ξ_{RX} under the same constraints. Therefore, the convex optimization problem for the cooperative MC system with the N-out-of-K rule in the perfect reporting scenario is formulated as

$$\begin{aligned} \min_{\xi_{\text{RX}}} \quad & P_1 Q_{\text{md}}^+[j] + (1 - P_1)Q_{\text{fa}}^+[j] \\ \text{s.t.} \quad & \text{(22) and (23).} \end{aligned} \tag{33}$$

We note that the convex optimization problem for the single-RX system in the perfect reporting scenario is a special case of problems (27), (29), and (33), with $K = 1$.

B. Noisy Reporting

In this subsection, we first extend the formulated convex optimization problems from the perfect reporting scenario to the noisy reporting scenario, assuming that ξ_{FC} is fixed. We then formulate the joint convex optimization problems with respect to *both* ξ_{RX} and ξ_{FC} for the OR rule, AND rule, and N-out-of-K rule.

1) Optimal ξ_{RX}: We first analyze the convexity of $\tilde{P}_{\text{md}}[j]^K$ and $\tilde{P}_{\text{fa}}[j]^K$ with respect to ξ_{RX}. To facilitate the convexity analysis of $\tilde{P}_{\text{md}}[j]^K$ and $\tilde{P}_{\text{fa}}[j]^K$ with respect to ξ_{RX}, we approximate (17) and (18) using (19), which result in

$$\begin{aligned} \tilde{P}_{\text{md}}[j] \approx \frac{1}{4} \big[& 2 + (1 + \Lambda(\xi_{\text{RX}}, U_1[j])) \Lambda(\xi_{\text{FC}}, V_0[j]) \\ & + (1 - \Lambda(\xi_{\text{RX}}, U_1[j])) \Lambda(\xi_{\text{FC}}, V_1[j]) \big] \end{aligned} \tag{34}$$

and

$$\begin{aligned} \tilde{P}_{\text{fa}}[j] \approx \frac{1}{4} \big[& 2 - (1 + \Lambda(\xi_{\text{RX}}, U_0[j])) \Lambda(\xi_{\text{FC}}, V_0[j]) \\ & + (-1 + \Lambda(\xi_{\text{RX}}, U_0[j])) \Lambda(\xi_{\text{FC}}, V_1[j]) \big], \end{aligned} \tag{35}$$

respectively. Recall that $V_{\tilde{z},k}[j]$, $\tilde{z} \in \{0, 1\}$, denotes the conditional mean of $S_{\text{ob},k}^{(\text{RX}_k,\text{FC})}[j]$ when the most recent information symbol transmitted by the RX_k is $\tilde{z}$. We find that $V_{\tilde{z}}[j]$ depends on $\hat{\mathbf{W}}_{\text{RX}_k}^{j-1}$ and $\hat{\mathbf{W}}_{\text{RX}_k}^{j-1}$ depends on ξ_{RX}. Thus, $V_{\tilde{z}}[j]$ depends on ξ_{RX}, which complicates the convexity analysis of $\tilde{P}_{\text{md}}[j]^K$ and $\tilde{P}_{\text{fa}}[j]^K$ with respect to ξ_{RX}. To avoid this complication, we consider a constant $V_{\tilde{z}}[j]$ in the jth symbol interval, denoted by $\overline{V}_{\tilde{z}}[j]$, which is averaged over all the

realizations of $\hat{\mathbf{W}}_{\text{RX}_k}^{j-1}$, to approximate $V_{\tilde{z}}[j]$ in (34) and (35)[7]. By doing so, we obtain $\overline{V}_{\tilde{z}}[j]$ as

$$\overline{V}_{\tilde{z}}[j] = \frac{1}{|\omega_j|} \sum_{\hat{\mathbf{W}}_{\text{RX}_k}^{j-1} \in \omega_j} V_{\tilde{z}}[j], \tag{36}$$

where ω_j is the set containing all realizations of $\hat{\mathbf{W}}_{\text{RX}_k}^{j-1}$ and $|\omega_j|$ denotes the cardinality of ω_j. Using $\overline{V}_{\tilde{z}}[j]$, we further approximate $\tilde{P}_{\text{md}}[j]$ and $\tilde{P}_{\text{fa}}[j]$ as [8]

$$\begin{aligned} \tilde{P}_{\text{md}}[j] \approx \frac{1}{4} \big[& 2 + (1 + \Lambda(\xi_{\text{RX}}, U_1[j])) \Lambda(\xi_{\text{FC}}, \overline{V}_0[j]) \\ & + (1 - \Lambda(\xi_{\text{RX}}, U_1[j])) \Lambda(\xi_{\text{FC}}, \overline{V}_1[j]) \big] \end{aligned} \tag{37}$$

and

$$\begin{aligned} \tilde{P}_{\text{fa}}[j] \approx \frac{1}{4} \big[& 2 - (1 + \Lambda(\xi_{\text{RX}}, U_0[j])) \Lambda(\xi_{\text{FC}}, \overline{V}_0[j]) \\ & + (-1 + \Lambda(\xi_{\text{RX}}, U_0[j])) \Lambda(\xi_{\text{FC}}, \overline{V}_1[j]) \big], \end{aligned} \tag{38}$$

respectively. We now present the conditions making $\tilde{P}_{\text{md}}[j]^K$ and $\tilde{P}_{\text{fa}}[j]^K$ convex in the following theorem.

Theorem 2: $\tilde{P}_{\text{md}}[j]^K$ and $\tilde{P}_{\text{fa}}[j]^K$ are convex with respect to ξ_{RX} when ξ_{FC} is fixed, if we impose the convex constraints (22) and (23), respectively.

Proof: We derive the second derivative of $\tilde{P}_{\text{md}}[j]^K$ as

$$\begin{aligned} \frac{\partial^2 \tilde{P}_{\text{md}}[j]^K}{\partial \xi_{\text{RX}}^2} = & (-0.5 - U_1[j] + \xi_{\text{RX}}) \Upsilon(K - 1, 1, 3/2) \\ & + (K - 1)\Upsilon(K - 2, 2, 1) \end{aligned} \tag{39}$$

where

$$\begin{aligned} \Upsilon(\alpha, \beta, \gamma) = & \Big[(1 + \Lambda(\xi_{\text{RX}}, U_1[j])) \left(1 + \Lambda(\xi_{\text{FC}}, \overline{V}_0[j])\right) \\ & + (1 - \Lambda(\xi_{\text{RX}}, U_1[j])) \left(1 + \Lambda(\xi_{\text{FC}}, \overline{V}_1[j])\right) \Big]^\alpha \\ & \times \left(\Lambda(\xi_{\text{FC}}, \overline{V}_1[j]) - \Lambda(\xi_{\text{FC}}, \overline{V}_0[j]) \right)^\beta \\ & \times \frac{K\Theta(\xi_{\text{RX}}, U_1[j])^\beta}{U_1[j]^\gamma 4^\alpha (2\sqrt{2\pi})^\beta}. \end{aligned} \tag{40}$$

We next examine the monotonicity of $\Lambda(\xi_{\text{FC}}, V)$ with respect to V, $V \in \{\overline{V}_{1,k}[j], \overline{V}_{0,k}[j]\}$. We derive the first derivative of $\Lambda(\xi_{\text{FC}}, \lambda)$ with respect to λ as

$$\frac{\partial \Lambda(\xi_{\text{FC}}, \lambda)}{\partial \lambda} = \frac{2\Theta(\xi_{\text{FC}}, \lambda)(-\xi_{\text{FC}} + 0.5 - \lambda)}{2\sqrt{2\pi}\lambda^{\frac{3}{2}}}. \tag{41}$$

Since $\Theta(\xi_{\text{FC}}, \lambda) > 0$ and $(-\xi_{\text{FC}} + 0.5 - \lambda) < 0$, we find that $\Lambda(\xi_{\text{FC}}, \lambda)$ is a monotonically decreasing function with respect to λ. Therefore, we have $\left(\Lambda(\xi_{\text{FC}}, \overline{V}_1[j]) - \Lambda(\xi_{\text{FC}}, \overline{V}_0[j])\right) \leq$

---

[7]We note that the occurrence likelihood of each realization of $\hat{\mathbf{W}}_{\text{RX}_k}^{j-1}$ may not be the same in practice, since it depends on the value of ξ_{RX}. For example, when ξ_{RX} is very high, $\hat{\mathbf{W}}_{\text{RX}_k}^{j-1}$ would be all "0"s, while when ξ_{RX} is very small, $\hat{\mathbf{W}}_{\text{RX}_k}^{j-1}$ would be all "1"s. In this paper, we assume an equal occurrence likelihood to keep a low evaluation complexity, but this does not have a significant impact on the analytical results.

[8]We clarify that we approximate $V_{\tilde{z}}[j]$ by $\overline{V}_{\tilde{z}}[j]$ in (34) and (35) to obtain (37) and (38) for the *convexity analysis*. This approximation is not for deriving the expected MDP and FAP of each $\text{TX} - \text{RX}_k - \text{FC}$ link in the jth symbol interval, i.e., $\tilde{P}_{\text{md},k}[j]$ and $\tilde{P}_{\text{fa},k}[j]$, since (34) and (35) are already the approximations of $\tilde{P}_{\text{md},k}[j]$ and $\tilde{P}_{\text{fa},k}[j]$, respectively.

0. It follows that (39) is always nonnegative if we impose the constraint (22), and thus $\tilde{P}_{\mathrm{md}}[j]^K$ is convex with respect to ξ_{RX}. Similarly, we prove that $\tilde{P}_{\mathrm{fa}}[j]^K$ is convex with respect to ξ_{RX}, if we impose the convex constraint (23). ∎

Similar to (26) and (28), we upper-bound $Q_{\mathrm{fa}}[j]$ for the OR rule and $Q_{\mathrm{md}}[j]$ for the AND rule as

$$Q_{\mathrm{fa}}[j] \leq K\tilde{P}_{\mathrm{fa}}[j] \tag{42}$$

and

$$Q_{\mathrm{md}}[j] \leq K\tilde{P}_{\mathrm{md}}[j], \tag{43}$$

respectively. We note that $\tilde{P}_{\mathrm{fa}}[j]$ and $\tilde{P}_{\mathrm{md}}[j]$ are convex with respect to ξ_{RX}, if we impose the constraints (22) and (23), respectively, which can be proven by considering $K = 1$ in Theorem 2. Since (42) and (43) scale a convex function with a nonnegative constant, they are also convex with respect to ξ_{RX} under the same constraints. Next, we focus on $Q_{\mathrm{md}}[j]$ for the OR rule and $Q_{\mathrm{fa}}[j]$ for the AND rule. Based on Theorem 2, we note that $\tilde{P}_{\mathrm{md}}[j]^K$ and $\tilde{P}_{\mathrm{fa}}[j]^K$ are convex with respect to ξ_{RX} when ξ_{FC} is fixed, if we impose the convex constraints (22) and (23), respectively. Then, we focus on the N-out-of-K rule. We note that $\tilde{P}_{\mathrm{md}}[j]^{\tilde{n}}$ and $\tilde{P}_{\mathrm{fa}}[j]^n$ are convex with respect to ξ_{RX} when ξ_{FC} is fixed, if we impose the convex constraints (22) and (23), respectively, which can be proven by replacing K with $\tilde{n}$ and n in Theorem 2, respectively. For the N-out-of-K rule, using a similar method to (30)–(32), we can derive the upper bounds on $Q_{\mathrm{md}}[j]$ and $Q_{\mathrm{fa}}[j]$ that are convex with respect to ξ_{RX}, given that $\tilde{P}_{\mathrm{md}}[j]^{\tilde{n}}$ and $\tilde{P}_{\mathrm{fa}}[j]^n$ are convex with respect to ξ_{RX}.

In the noisy reporting scenario, we formulate the convex optimization problems with respect to ξ_{RX} given fixed ξ_{FC} for the OR rule, AND rule, and N-out-of-K rule by replacing $P_{\mathrm{md}}[j]$ and $P_{\mathrm{fa}}[j]$ with $\tilde{P}_{\mathrm{md}}[j]$ and $\tilde{P}_{\mathrm{fa}}[j]$, respectively, in (27), (29), and (33). We note that the convex optimization problem with respect to ξ_{RX_k} for the single-RX system in the noisy reporting scenario is a special case of the corresponding problem for a cooperative MC system with $K = 1$.

2) Joint Optimal ξ_{RX} and ξ_{FC}: We first analyze the joint convexity of $\tilde{P}_{\mathrm{md}}[j]^K$ and $\tilde{P}_{\mathrm{fa}}[j]^K$ with respect to ξ_{RX} and ξ_{FC}. To facilitate the joint convexity analysis of $\tilde{P}_{\mathrm{md}}[j]^K$ and $\tilde{P}_{\mathrm{fa}}[j]^K$ with respect to both ξ_{RX} and ξ_{FC}, we consider the approximations given by

$$\Pr\left(S_{\mathrm{ob},k}^{(\mathrm{RX}_k,\mathrm{FC})}[j] < \xi_{\mathrm{FC}}\middle|\hat{W}_{\mathrm{RX}_k}[j] = 0, \hat{\mathbf{W}}_{\mathrm{RX}_k}^{j-1}\right) \approx 1 \tag{44}$$

and

$$\Pr\left(S_{\mathrm{ob},k}^{(\mathrm{RX}_k,\mathrm{FC})}[j] \geq \xi_{\mathrm{FC}}\middle|\hat{W}_{\mathrm{RX}_k}[j] = 1, \hat{\mathbf{W}}_{\mathrm{RX}_k}^{j-1}\right) \approx 1, \tag{45}$$

which are tight when the error probability of the $\mathrm{RX}_k - \mathrm{FC}$ link is low. We emphasize that we still keep

$$\Pr\left(S_{\mathrm{ob},k}^{(\mathrm{RX}_k,\mathrm{FC})}[j] < \xi_{\mathrm{FC}}\middle|\hat{W}_{\mathrm{RX}_k}[j] = 1, \hat{\mathbf{W}}_{\mathrm{RX}_k}^{j-1}\right) \tag{46}$$

and

$$\Pr\left(S_{\mathrm{ob},k}^{(\mathrm{RX}_k,\mathrm{FC})}[j] \geq \xi_{\mathrm{FC}}\middle|\hat{W}_{\mathrm{RX}_k}[j] = 0, \hat{\mathbf{W}}_{\mathrm{RX}_k}^{j-1}\right) \tag{47}$$

in (37) and (38), respectively. Employing (44) and (45) into (37) and (38), respectively, we further upper-bound $\tilde{P}_{\mathrm{md}}[j]$ and $\tilde{P}_{\mathrm{fa}}[j]$ as

$$\tilde{P}_{\mathrm{mdb}}[j] = \frac{1}{4}\left[3 + \Lambda\left(\xi_{\mathrm{RX}}, U_1[j]\right)\right.$$
$$\left. + \left(1 - \Lambda\left(\xi_{\mathrm{RX}}, U_1[j]\right)\right)\Lambda\left(\xi_{\mathrm{FC}}, \overline{V}_1[j]\right)\right] \tag{48}$$

and

$$\tilde{P}_{\mathrm{fab}}[j] = \frac{1}{4}\left[3 - \Lambda\left(\xi_{\mathrm{FC}}, \overline{V}_0[j]\right)\right.$$
$$\left. - \left(1 + \Lambda\left(\xi_{\mathrm{FC}}, \overline{V}_0[j]\right)\right)\Lambda\left(\xi_{\mathrm{RX}}, U_0[j]\right)\right], \tag{49}$$

respectively, where $\tilde{P}_{\mathrm{mdb}}[j]$ and $\tilde{P}_{\mathrm{fab}}[j]$ are the upper bounds on $\tilde{P}_{\mathrm{md}}[j]$ and $\tilde{P}_{\mathrm{fa}}[j]$, respectively. We now present the constraints making $\tilde{P}_{\mathrm{mdb}}[j]^K$ and $\tilde{P}_{\mathrm{fab}}[j]^K$ convex in the following two theorems.

Theorem 3: $\tilde{P}_{\mathrm{mdb}}[j]^K$ is jointly convex with respect to ξ_{RX} and ξ_{FC}, if we impose the convex constraints (22), and the following constraints:

$$-0.5 - \overline{V}_1[j] + \xi_{\mathrm{FC}} \leq 0, \tag{50}$$

$$\Phi\left(\xi_{\mathrm{RX}}, \xi_{\mathrm{FC}}^+, K\right) \leq 0, \text{ and } \Phi\left(\xi_{\mathrm{RX}}^+, \xi_{\mathrm{FC}}, K\right) \leq 0, \tag{51}$$

where ξ_{RX}^- and ξ_{RX}^+ are bounds on ξ_{RX}, and ξ_{FC}^- and ξ_{FC}^+ are bounds on ξ_{FC}, and $\Phi\left(\mu, \nu, K\right)$ is given in (52) at the top of page 10.

Theorem 4: $\tilde{P}_{\mathrm{fab}}[j]^K$ is jointly convex with respect to ξ_{RX} and ξ_{FC}, if we impose the convex constraints (23) and the following constraints:

$$0.5 + \overline{V}_0[j] - \xi_{\mathrm{FC}} \leq 0, \tag{53}$$

$$\Psi\left(\xi_{\mathrm{RX}}, \xi_{\mathrm{FC}}^-, K\right) \leq 0, \text{ and } \Psi\left(\xi_{\mathrm{RX}}^-, \xi_{\mathrm{FC}}, K\right) \leq 0, \tag{54}$$

where $\Psi\left(\mu, \nu, K\right)$ is given in (55) at the top of page 10.

Proof: The proof of Theorem 3 and Theorem 4 is given in the Appendix. ∎

Similar to (26) and (28), we upper-bound $Q_{\mathrm{fa}}[j]$ for the OR rule and $Q_{\mathrm{md}}[j]$ for the AND rule as

$$Q_{\mathrm{fa}}[j] \leq K\tilde{P}_{\mathrm{fab}}[j] \tag{56}$$

and

$$Q_{\mathrm{md}}[j] \leq K\tilde{P}_{\mathrm{mdb}}[j], \tag{57}$$

respectively. We note that $\tilde{P}_{\mathrm{fab}}[j]$ is convex with respect to ξ_{RX} and ξ_{FC}, if we impose the constraints (23), (53), $\Psi\left(\xi_{\mathrm{RX}}, \xi_{\mathrm{FC}}^-, 1\right) \leq 0$, and $\Psi\left(\xi_{\mathrm{RX}}^-, \xi_{\mathrm{FC}}, 1\right) \leq 0$, which can be proven by considering $K = 1$ in Theorem 4. We also note that $\tilde{P}_{\mathrm{mdb}}[j]$ is convex with respect to ξ_{RX} and ξ_{FC}, if we impose the constraints (22), (50), $\Phi\left(\xi_{\mathrm{RX}}, \xi_{\mathrm{FC}}^+, 1\right) \leq 0$, and $\Phi\left(\xi_{\mathrm{RX}}^+, \xi_{\mathrm{FC}}, 1\right) \leq 0$, which can be proven by considering $K = 1$ in Theorem 3. Since (56) and (57) scale a convex function with a nonnegative constant, they are also convex with respect to ξ_{RX} and ξ_{FC} under the same constraints. We then focus on the joint convexity analysis of $Q_{\mathrm{md}}[j]$ for the OR rule and $Q_{\mathrm{fa}}[j]$ for the AND rule. Based on Theorem 3 and Theorem 4, we note that $\tilde{P}_{\mathrm{mdb}}[j]^K$ and $\tilde{P}_{\mathrm{fab}}[j]^K$ are jointly convex with respect to ξ_{RX} and ξ_{FC}, respectively. For the N-out-of-K rule, we note that $\tilde{P}_{\mathrm{mdb}}[j]^{\tilde{n}}$ is jointly convex with respect to ξ_{RX}

$$\Phi\left(\mu,\nu,K\right) = 4\Theta\left(\xi_{\text{RX}}^+, U_1[j]\right)\left(-4 + K + K\Lambda\left(\xi_{\text{FC}}^-, \overline{V}_1[j]\right) + K\Lambda\left(\xi_{\text{RX}}^-, U_1[j]\right)\left(1 + \Lambda\left(\xi_{\text{FC}}^-, \overline{V}_1[j]\right)\right)\right)^2 - \frac{\left(1 + \Lambda\left(\xi_{\text{RX}}^-, U_1[j]\right)\right)}{\sqrt{U_1[j]\overline{V}_1[j]}}$$

$$\times\left(1 + \Lambda\left(\xi_{\text{FC}}^-, \overline{V}_1[j]\right)\right)\left(2\left(-1 + K\right)\sqrt{\overline{V}_1[j]}\left(1 + \Lambda\left(\xi_{\text{RX}}^+, U_1[j]\right)\right) - \frac{\sqrt{2\pi}}{\Theta\left(\xi_{\text{FC}}^+, \overline{V}_1[j]\right)}\left(0.5 + \overline{V}_1[j] - \nu\right)\right)$$

$$\times\left(-3 + \Lambda\left(\xi_{\text{FC}}^+, \overline{V}_1[j]\right) + \Lambda\left(\xi_{\text{RX}}^+, U_1[j]\right)\left(1 + \Lambda\left(\xi_{\text{FC}}^+, \overline{V}_1[j]\right)\right)\right)\left(\Theta\left(\xi_{\text{RX}}^+, U_1[j]\right)\left(1 + \Lambda\left(\xi_{\text{FC}}^-, \overline{V}_1[j]\right)\right)\right)$$

$$\times\left(-1 + K\right)2\sqrt{U_1[j]} - \sqrt{2\pi}\left(0.5 + U_1[j] - \mu\right)\left(-3 + \Lambda\left(\xi_{\text{FC}}^+, \overline{V}_1[j]\right) + \Lambda\left(\xi_{\text{RX}}^+, U_1[j]\right)\left(1 + \Lambda\left(\xi_{\text{FC}}^+, \overline{V}_1[j]\right)\right)\right)\right) \quad (52)$$

$$\Psi\left(\mu,\nu,K\right) = 4\Theta\left(\xi_{\text{RX}}^-, U_0[j]\right)\left(-4 + K - K\Lambda\left(\xi_{\text{FC}}^+, \overline{V}_0[j]\right) + K\Lambda\left(\xi_{\text{RX}}^+, U_0[j]\right)\left(-1 + \Lambda\left(\xi_{\text{FC}}^+, \overline{V}_0[j]\right)\right)\right)^2 - \frac{\left(1 - \Lambda\left(\xi_{\text{RX}}^+, U_0[j]\right)\right)}{\sqrt{U_0[j]\overline{V}_0[j]}}$$

$$\times\left(-1 + \Lambda\left(\xi_{\text{FC}}^-, \overline{V}_0[j]\right)\right)\left(-2\left(-1 + K\right)\sqrt{\overline{V}_0[j]}\left(-1 + \Lambda\left(\xi_{\text{RX}}^-, U_0[j]\right)\right) + \frac{\sqrt{2\pi}}{\Theta\left(\xi_{\text{FC}}^-, \overline{V}_0[j]\right)}\left(0.5 + \overline{V}_0[j] - \nu\right)\right)$$

$$\times\left(-3 - \Lambda\left(\xi_{\text{FC}}^+, \overline{V}_0[j]\right) + \Lambda\left(\xi_{\text{RX}}^-, U_0[j]\right)\left(-1 + \Lambda\left(\xi_{\text{FC}}^-, \overline{V}_0[j]\right)\right)\right)\left(\Theta\left(\xi_{\text{RX}}^-, U_0[j]\right)\left(-1 + \Lambda\left(\xi_{\text{FC}}^-, \overline{V}_0[j]\right)\right)\right)$$

$$\times\left(-1 + K\right)2\sqrt{U_0[j]} - \sqrt{2\pi}\left(0.5 + U_0[j] - \mu\right)\left(-3 - \Lambda\left(\xi_{\text{FC}}^-, \overline{V}_0[j]\right) + \Lambda\left(\xi_{\text{RX}}^-, U_0[j]\right)\left(-1 + \Lambda\left(\xi_{\text{FC}}^+, \overline{V}_0[j]\right)\right)\right)\right) \quad (55)$$

---

and ξ_{FC} under the constraints (22), (50), $\Phi\left(\xi_{\text{RX}}, \xi_{\text{FC}}^+, \tilde{n}\right) \leq 0$, and $\Phi\left(\xi_{\text{RX}}^+, \xi_{\text{FC}}, \tilde{n}\right) \leq 0$, which can be proven by replacing K with $\tilde{n}$ in Theorem 3. We also note that $\tilde{P}_{\text{fab}}[j]^n$ is jointly convex with respect to ξ_{RX} and ξ_{FC} under the constraints (23), (53), $\Psi\left(\xi_{\text{RX}}, \xi_{\text{FC}}^-, n\right) \leq 0$, and $\Psi\left(\xi_{\text{RX}}^-, \xi_{\text{FC}}, n\right) \leq 0$, which can be proven by replacing K with n in Theorem 4. Given that $\tilde{P}_{\text{mdb}}[j]^n$ and $\tilde{P}_{\text{fab}}[j]^n$ are jointly convex with respect to ξ_{RX} and ξ_{FC} and applying a similar method to (30)–(32), we can derive the upper bounds on $Q_{\text{md}}[j]$ and $Q_{\text{fa}}[j]$ which are jointly convex with respect to ξ_{RX} and ξ_{FC}.

In the noisy reporting scenario, we formulate the convex optimization problems with respect to ξ_{RX} and ξ_{FC} for the OR rule, AND rule, and N-out-of-K rule as

$$\min_{\xi_{\text{RX}}, \xi_{\text{FC}}} \quad P_1\tilde{P}_{\text{mdb}}[j]^K + \left(1 - \tilde{P}_1\right)KP_{\text{fab}}[j]$$
$$\text{s.t.} \quad (22), (23), (50) - (53), \quad (58)$$
$$\Psi\left(\xi_{\text{RX}}, \xi_{\text{FC}}^-, 1\right) \leq 0, \text{ and } \Psi\left(\xi_{\text{RX}}^-, \xi_{\text{FC}}, 1\right) \leq 0,$$

$$\min_{\xi_{\text{RX}}, \xi_{\text{FC}}} \quad P_1K\tilde{P}_{\text{mdb}}[j] + \left(1 - P_1\right)\tilde{P}_{\text{fab}}[j]^K$$
$$\text{s.t.} \quad (22), (23), (50), (53), (54), \quad (59)$$
$$\Phi\left(\xi_{\text{RX}}, \xi_{\text{FC}}^+, 1\right) \leq 0, \text{ and } \Phi\left(\xi_{\text{RX}}^+, \xi_{\text{FC}}, 1\right) \leq 0,$$

and

$$\min_{\xi_{\text{RX}}, \xi_{\text{FC}}} \quad P_1\tilde{Q}_{\text{md}}^+[j] + (1 - P_1)\tilde{Q}_{\text{fa}}^+[j]$$
$$\text{s.t.} \quad (22), (23), (50), (53),$$
$$\Phi\left(\xi_{\text{RX}}^+, \xi_{\text{FC}}, \tilde{n}\right) \leq 0, \ \Phi\left(\xi_{\text{RX}}, \xi_{\text{FC}}^+, \tilde{n}\right) \leq 0, \quad (60)$$
$$\Psi\left(\xi_{\text{RX}}, \xi_{\text{FC}}^-, n\right) \leq 0, \text{ and } \Psi\left(\xi_{\text{RX}}^-, \xi_{\text{FC}}, n\right) \leq 0,$$

respectively, where $\tilde{Q}_{\text{md}}^+[j] \triangleq \sum_{\tilde{n}=K-N+1}^K \binom{K}{\tilde{n}}\tilde{P}_{\text{mdb}}[j]^{\tilde{n}}$ and $\tilde{Q}_{\text{fa}}^+[j] \triangleq \sum_{n=N}^K \binom{K}{n}\tilde{P}_{\text{fab}}[j]^n$. We emphasize that the constraints $\Phi\left(\xi_{\text{RX}}^+, \xi_{\text{FC}}, \tilde{n}\right) \leq 0$, $\Phi\left(\xi_{\text{RX}}, \xi_{\text{FC}}^+, \tilde{n}\right) \leq 0$, $\Psi\left(\xi_{\text{RX}}, \xi_{\text{FC}}^-, n\right) \leq 0$, $\Psi\left(\xi_{\text{RX}}^-, \xi_{\text{FC}}, n\right) \leq 0$ for each $\tilde{n}$ and n

are applied in (60), where $\tilde{n} \in \{K - N + 1, \ldots, K\}$ and $n \in \{N, \ldots, K\}$, to ensure the convexity of $\tilde{Q}_{\text{md}}^+[j]$ and $\tilde{Q}_{\text{fa}}^+[j]$. We note that the jointly convex optimization problem for the single-RX system in the noisy reporting scenario is a special case of problems (58), (59), and (60), with $K = 1$.

C. Average Error Performance Optimization

We emphasize that the solutions to the formulated optimization problems in Sections IV-A and IV-B are the *instantaneous* suboptimal thresholds which minimize the instantaneous system error performance for given $\mathbf{W}_{\text{TX}}^{j-1}$. As previously explained, it may not be realistic for the RXs and FC to calculate the instantaneous suboptimal thresholds and such calculation incurs significant computational overhead. Therefore, in this subsection we aim to obtain a *single* suboptimal threshold which optimizes the average system error performance over all possible realizations of $\mathbf{W}_{\text{TX}}^{j-1}$ and across all symbol intervals.

If we aim to optimize $\overline{Q}_{\text{FC}}$ for the OR rule in the perfect reporting scenario, based on (27), then we formulate the problem as

$$\underset{\xi_{\text{RX}}}{\text{minimize}} \quad \frac{1}{L}\sum_{j=1}^L\left(\frac{1}{|\omega_j|}\sum_{\omega_j}P_{\text{md}}[j]^K + KP_{\text{fa}}[j]\right)$$
$$\text{s.t.} \quad \text{all constraints for all considered realizations}$$
$$\text{of } \mathbf{W}_{\text{TX}}^{j-1} \text{ in } \omega_j \text{ for each symbol interval.}$$
$$(61)$$

The empirical average error performance of the system is optimized in (61), since we assume that the occurrence likelihoods of the realizations of $\mathbf{W}_{\text{TX}}^{j-1}$ are equal. Using a formulation similar to (61), we can extend all convex optimization problems for optimizing the instantaneous system error performance to those for optimizing the average system error performance. Also, since all the derived inequality constraint

functions are affine, the constraints define the lower limits and upper limits on ξ_{RX} and/or ξ_{FC}. We clarify that it is reasonable to only consider the minimum upper limit and the maximum lower limit on ξ_{RX} and/or ξ_{FC} among all the upper and lower limits.

V. NUMERICAL RESULTS AND SIMULATIONS

In this section, we present numerical and simulation results to examine the error performance of the cooperative MC system. The simulation results are generated by a particle-based stochastic simulator, where we track the precise locations of all individual molecules over discrete time steps. We clarify that all the approximations in Sections III and IV are only considered for facilitating our theoretical analysis, i.e., the theoretical evaluation and optimization of error performance. We do not adopt these approximations in our simulations. In our simulations, we consider a cooperative system as described in Section II. In this section, we also demonstrate the effectiveness of the solutions to our formulated convex optimization problems, referred to as suboptimal solutions, by comparing them with the actual optimal solutions that minimize the expected average error probability of the system. We use the fmincon solver in MATLAB with the interior-point algorithm to obtain the suboptimal solutions. We clarify that the actual optimal solutions are obtained via the exhaustive search of the numerical results of the expected *average* error probability. Such solutions *do not* require the information of $\mathbf{W}_{\mathrm{TX}}^{j-1}$. We denote $\xi_{\mathrm{RX}}^{\circ}$ and $\xi_{\mathrm{FC}}^{\circ}$ as suboptimal solutions and denote ξ_{RX}^{*} and ξ_{FC}^{*} as actual optimal solutions. We refer to the minimum upper bounds achieved by $\xi_{\mathrm{RX}}^{\circ}$ and $\xi_{\mathrm{FC}}^{\circ}$ as suboptimal error probabilities. We refer to the expected error probability achieved by $\xi_{\mathrm{RX}}^{\circ}$ and $\xi_{\mathrm{FC}}^{\circ}$ as the approximated error probabilities.

We list all the fixed environmental parameters adopted in this section in Table I. The varying parameters adopted in this section are the decision threshold at RXs, ξ_{RX}, the decision threshold at the FC, ξ_{FC}, the number of RXs, K, the radius of RX_k, r_{RX_k}, and the radius of the FC, r_{FC}. In particular, r_{RX_k} is set as $0.225\,\mu\mathrm{m}$ in all the figures except for Fig. 3 and r_{FC} is fixed at $0.2\,\mu\mathrm{m}$ in all the figures except for Fig. 6. In Fig. 3, we set r_{RX_k} as $0.2\,\mu\mathrm{m}$. In the following, we assume that the TX releases $S_0 = 8000$ molecules for information symbol "1" and the total number of molecules released by all RXs for symbol "1" is fixed at 2000, i.e., each RX releases $S_k = 2000/K$ molecules to report its decision of symbol "1". The locations of the TX, RXs, and FC are listed in Table II. For each realization of $\mathbf{W}_{\mathrm{TX}}^{j-1}$, we set $\xi_{\mathrm{RX}}^{-} = U_0[j]+1$, $\xi_{\mathrm{RX}}^{+} = U_1[j]$, $\xi_{\mathrm{FC}}^{-} = \overline{V}_0[j] + 1$, and $\xi_{\mathrm{FC}}^{+} = \overline{V}_1[j]$, since the initial convex feasible sets of ξ_{RX} and ξ_{FC} are $0.5+U_0[j] \le \xi_{\mathrm{RX}} \le 0.5+U_1[j]$ and $0.5 + \overline{V}_0[j] \le \xi_{\mathrm{FC}} \le 0.5 + \overline{V}_1[j]$, respectively.

Throughout this section, $\overline{Q}_{\mathrm{FC}}$ are calculated by averaging $P_{\mathrm{e},k}[j]$ and $Q_{\mathrm{FC}}[j]$, respectively, over all considered realizations of $\mathbf{W}_{\mathrm{TX}}^{j-1}$ and across all symbol intervals. Here, we consider all possible realizations of $\mathbf{W}_{\mathrm{TX}}^{j-1}$ except for the realization of all "0" bits, i.e., when the MDP is zero and there is no optimal threshold. Since we consider the length of the symbol sequence from the TX is 10 bits, we consider 1023 different symbol sequences in total. The simulated error probabilities

Parameter	Symbol	Value
Radius of RXs	r_{RX_k}	$\{0.225\,\mu\mathrm{m}, 0.2\,\mu\mathrm{m}\}$
Radius of FC	r_{FC}	$0.2\,\mu\mathrm{m}$
Time step at RXs	Δt_{RX}	$100\,\mu\mathrm{s}$
Time step at FC	Δt_{FC}	$30\,\mu\mathrm{s}$
Number of samples of RXs	M_{RX}	5
Number of samples of FC	M_{FC}	5
Transmission time interval	t_{trans}	1 ms
Report time interval	t_{report}	0.3 ms
Bit interval time	T	1.3 ms
Diffusion coefficient	$D_0 = D_k$	$5 \times 10^{-9}\mathrm{m}^2/\mathrm{s}$
Length of symbol sequence	L	10
Probability of binary 1	P_1	0.5

TABLE II
LOCATIONS OF TX, RXs, AND FC

Devices	X-axis [μm]	Y-axis [μm]	Z-axis [μm]
TX	0	0	0
RX_1	2	0.6	0
RX_2	2	-0.6	0
RX_3	2	-0.3	0.5196
RX_4	2	-0.3	-0.519
RX_5	2	0.3	0.5196
RX_6	2	0.3	-0.5196
FC	2	0	0

are averaged over at least 5×10^4 independent transmissions of the considered symbol sequences. In Figs. 2–4, we plot the simulation for the expected error probabilities, while in Fig. 6, we plot the simulation for the approximated error probabilities. Moreover, we clarify that $\xi_{\mathrm{RX}}^{\circ}$ and $\xi_{\mathrm{FC}}^{\circ}$ for the expected average error probabilities are obtained using the optimization method in Section IV-C only *once* for all considered realizations of $\mathbf{W}_{\mathrm{TX}}^{j-1}$ and across all symbol intervals, unless otherwise noted. In other words, suboptimal solutions *do not* require the information of $\mathbf{W}_{\mathrm{TX}}^{j-1}$, unless otherwise noted. Furthermore, we clarify that the noninteger optimization solutions are rounded to integers in Figs. 3, 5, and 6. Specifically, the most two nearest integers around the solution are compared and the one achieving the lower error probability is chosen.

A. Perfect Reporting

In this subsection we consider the *perfect* reporting scenario. In Fig. 2, we consider a three-RX cooperative system and plot the average global error probability versus the decision threshold at the RXs for the OR rule, AND rule, and majority rule. The expected curves for the three rules are obtained from (8)–(13) with (5) and (6). The Gaussian approximation curves for the three rules are obtained from (8)–(13) with (20) and (21). The upper bound curves for the OR rule, AND rule, and majority rule are obtained from (10) and (26), (13) and (28), and (31) and (32), respectively, with (20) and (21). The value of $\xi_{\mathrm{RX}}^{\circ}$ for the OR rule, AND rule, and majority rule is obtained by solving (27), (29), and (33), respectively, with (20) and (21).

In Fig. 2, we first observe that the simulated points accurately match the expected curves, validating our analysis of
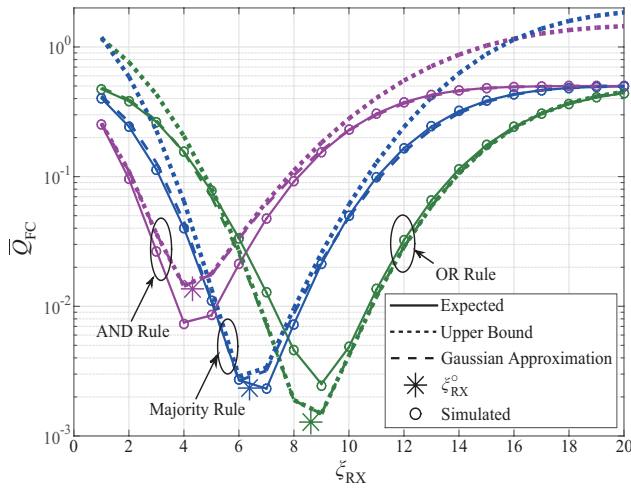
Fig. 2. Average global error probability $\overline{Q}_{FC}$ of different fusion rules versus the decision threshold at RXs ξ_{RX} with $K=3$ in the perfect reporting scenario.
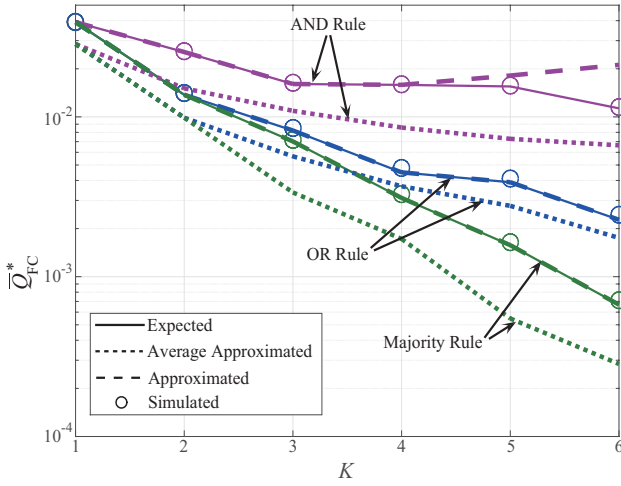

Fig. 3. Optimal average global error probability $\overline{Q}_{FC}^*$ of different fusion rules versus the number of cooperative RXs K in the perfect reporting scenario.

the expected results. Second, we observe that ξ_{RX}° is almost identical to ξ_{RX}^* for each fusion rule, confirming the accuracy of ξ_{RX}°. Third, we observe that the Gaussian approximation curves well approximate the expected curves. Fourth, we observe that the convex upper bound curve for the OR rule is lower than its expected curve. This can be explained as follows: In the single-RX system, the Gaussian approximations give an upper bound on $P_{md}[j]$ and a lower bound on $P_{fa}[j]$. For the OR rule, $Q_{md}[j]$ is the product of $P_{md}[j]$ and $Q_{fa}[j]$ is the sum of $P_{fa}[j]$. Since the Gaussian approximation of $Q_{md}[j]$ is tighter than that of $Q_{fa}[j]$, the Gaussian approximation of the global error probability for the OR rule is lower than the expected curve. Finally, observing the expected curves, we find that the majority rule outperforms the OR rule and the OR rule outperforms the AND rule at their corresponding optimal decision thresholds.

In Fig. 3, we plot the optimal average global error probability versus the number of cooperative RXs for the OR, AND, and majority rules. The baseline case is a single TX − RX link with $K = 1$, i.e., only one RX exists but no FC exists.

In the baseline case, we assume that the RX is located at $(2\,\mu m, 0.6\,\mu m, 0)$, the TX releases 10000 molecules, the time step between two successive samples is $100\,\mu s$, and the symbol interval time is $T = 1.3\,ms$, all of which ensure the fairness of the error performance comparison between the baseline case and the considered cooperative MC system. We keep the total number of molecules released by all RXs fixed for the fairness of error performance comparison between the baseline case and the cooperative MC system with different K. Moreover, the fixed total number of molecules applies to realistic biological environments where the number of available molecules within the environment may be limited. Also, for a fair comparison of different K, we consider that all RXs sample at the same time and has the same number of samples for different K, since the sampling time $t_{RX}(j, m)$ determines the mean number of molecules observed, based on (2) and (14). The value of $\overline{Q}_{FC}^*$ for each K in the expected curves for the three fusion rules is the minimum $\overline{Q}_{FC}$. For the expected curves, we consider that a single ξ_{RX}^* is applied to all considered realizations of $\mathbf{W}_{TX}^{j-1}$, which are obtained via exhaustive search of the expected expressions of (8)–(13) with (5) and (6). On the other hand, the value of $\overline{Q}_{FC}^*$ for each K in the approximated curves for the OR rule, AND rule, and majority rule are obtained by solving the corresponding average error performance optimization problems given by (27), (29), and (33), respectively. To this end, we use a single ξ_{RX}° for *all* considered realizations of $\mathbf{W}_{TX}^{j-1}$, and then calculate the actual values of $\overline{Q}_{FC}$ achieved by ξ_{RX}°. The value of $\overline{Q}_{FC}^*$ for each K in the *average* approximated curves are obtained by solving (27), (29), and (33), respectively, with (20) and (21) for all considered realizations. For this purpose, we consider a single ξ_{RX}° for *each* realization of $\mathbf{W}_{TX}^{j-1}$. Hence, for average approximated curves, the information of $\mathbf{W}_{TX}^{j-1}$ is required for suboptimal solutions. We then calculate the actual value of $Q_{FC}[j]$ achieved by ξ_{RX}° for each realization of $\mathbf{W}_{TX}^{j-1}$, and refer to it as the instantaneous approximated error probabilities. Finally, we calculate the mean of all the instantaneous approximated error probabilities for all realizations of $\mathbf{W}_{TX}^{j-1}$.

In Fig. 3, we first observe that for the OR rule and majority rule, the approximated curves match the expected curves, which confirms the accuracy of ξ_{RX}°. Second, we observe that for the AND rule, the approximated curve deviates from the expected curve when $K = 5$ and $K = 6$. This is due to the fact that ξ_{RX}° is outside the feasible set restricted by all the constraints for all realizations of $\mathbf{W}_{TX}^{j-1}$. Third, we observe an accurate match between the simulated points and the expected curves. Fourth, we observe that for the three fusion rules, the error performance clearly improves when the optimization is performed for each realization of $\mathbf{W}_{TX}^{j-1}$. However, as previously explained, this performance gain may not be feasible in practice and thus, we consider the average approximated curves as the best performance bound of our considered system. Fifth, we observe from the expected curves that the majority rule outperforms the OR rule and AND rule, which is consistent with that in Fig. 2. Lastly, we observe that the cooperative MC system outperforms the baseline case for all fusion rules, even though the distance of the baseline case is shorter than that of the cooperative MC
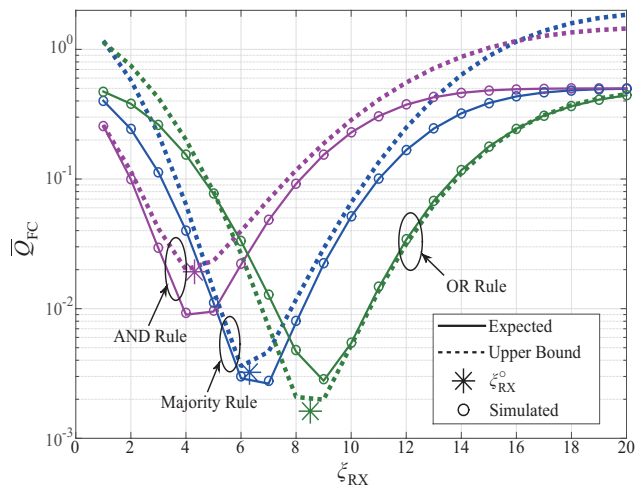
Fig. 4. Average global error probability $\overline{Q}_{FC}$ of different fusion rules versus the decision threshold at RXs ξ_{RX} with $K = 3$ in the noisy reporting scenario.

system. Importantly, we see that the system error performance significantly improves as K increases. This is due to fact that an increasing number of cooperative RXs enables more independent observations of the transmitted information symbol. It follows that the probability that all RXs fail to detect the transmitted information symbol is reduced.

We clarify that if we keep the *total volume* of all RXs fixed, then the system error performance degrades as K increases[9]. We note that a single TX-RX link with one RX has the same error performance as our simple soft fusion rule proposed in [1], since both schemes have the same mean number of molecules observed under the assumption of uniform concentration. In simple soft fusion, the FC adds all RXs' observations in the jth symbol interval and then compares it with a decision threshold ξ_{FC} to make a decision $\hat{W}_{FC}[j]$ (see [1]). We then note that the simple soft fusion rule outperforms the majority rule, since local hard decisions are a quantization that decreases the granularity of the information available to the FC. Thus, for a fixed total volume of RXs, the single TX-RX link outperforms the majority rule.
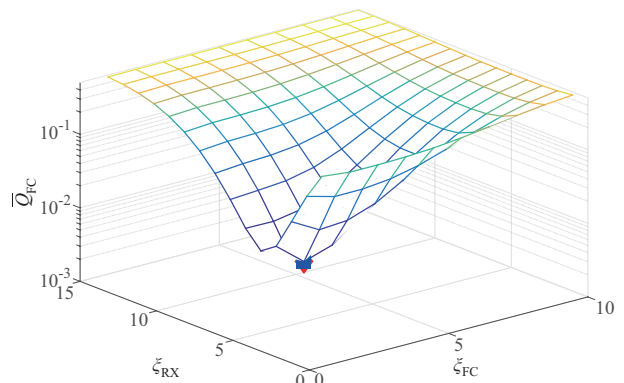
B. Noisy Reporting

In this subsection we focus on the *noisy* reporting scenario. In Fig. 4, we consider a three-RX cooperative system and plot the average global error probability versus the decision threshold at the RXs for the AND rule, OR rule, and majority rule. In this figure, we consider $\xi_{FC} = 2$ for the AND rule, $\xi_{FC} = 4$ for the OR rule, and $\xi_{FC} = 3$ for the majority rule, since these thresholds are the values obtained when the thresholds at the RXs and FC are jointly optimized for the three fusion rules. All curves in this figure are obtained from the same expressions and the same optimization problems as those in Fig. 2, except for replacing (5), (6), (20), and (21) with (17), (18), (37), and (38), respectively. Similar to Fig. 2, we observe that ξ_{RX}° is almost identical to ξ_{RX}^*. By comparing Fig. 2 with Fig. 4, we also observe that the expected error probabilities in Fig. 2 are
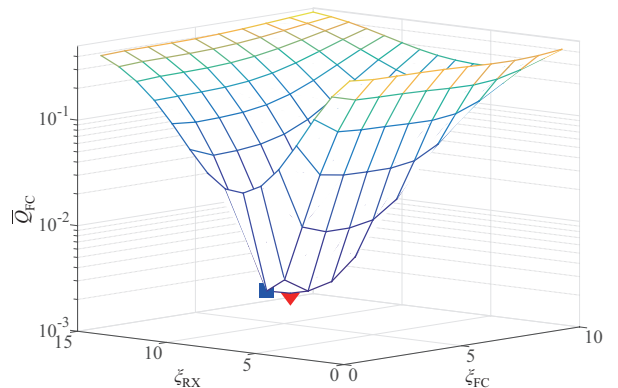
[9]For more details about this clarification, please refer to [31].
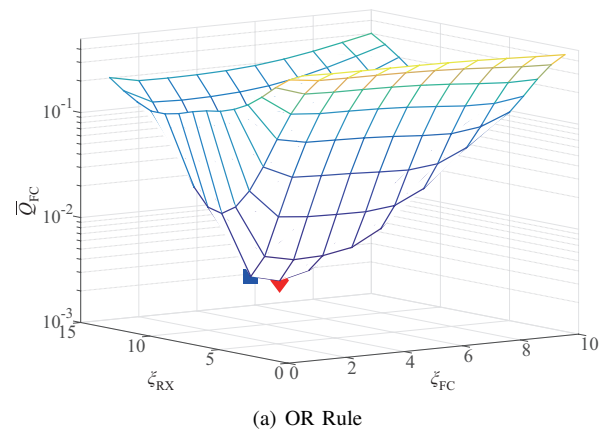
(a) OR Rule

(b) AND Rule

(c) Majority Rule

Fig. 5. Expected average global error probability $\overline{Q}_{FC}$ versus the decision threshold at RXs ξ_{RX} and the decision threshold at the FC ξ_{FC} with $K = 3$ in the noisy reporting scenario for (a) OR rule, (b) AND rule, and (c) majority rule. In (a)–(c), '♦' is the optimal $\overline{Q}_{FC}$ achieved by ξ_{RX}^* and ξ_{FC}^*, obtained by exhaustive search, and '■' is the approximated $\overline{Q}_{FC}$ achieved by ξ_{RX}° and ξ_{FC}°.

slightly lower than those in Fig. 4. We further observe that the optimal threshold at RXs is the same in Fig. 2 and Fig. 4. This observation is not surprising, since the relatively short distance between RX_k and the FC, which leads to a relatively low error probability in the $RX_k - FC$ link. This low error probability does not significantly affect the error probability of the $TX - RX_k - FC$ link. In addition, we also confirmed that increasing K significantly improves the system error performance in the noisy reporting scenario (figure omitted for brevity).

In Fig. 5, we consider a three-RX cooperative system and plot the expected average global error probability versus the

TABLE III
COORDINATES AND VALUES OF '♦' AND '■' IN FIG. 5

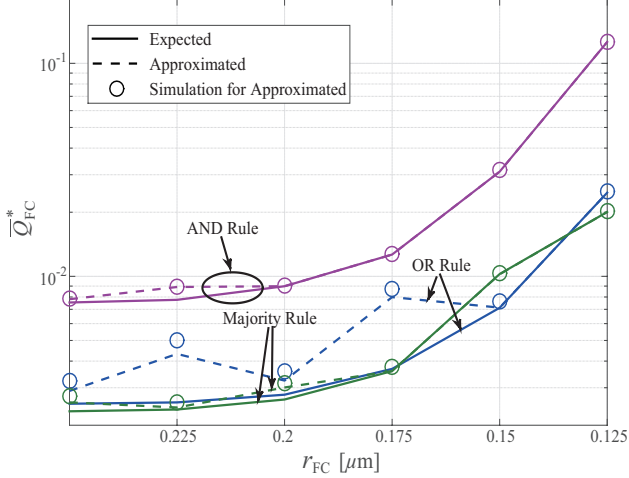| Variable	OR Rule	AND rule	Majority Rule
ξ_{FC}^* of '♦'	4	2	3
ξ_{RX}^* of '♦'	9	4	7
ξ_{FC}° of '■'	3	2	2
ξ_{RX}° of '■'	9	4	7
Value of '♦'	2.78×10^{-3}	8.99×10^{-3}	2.64×10^{-3}
Value of '■'	3.22×10^{-3}	8.99×10^{-3}	3.01×10^{-3}

Fig. 6. Optimal average global error probability $\overline{Q}_{FC}$ of different fusion rules versus the radius of the FC r_{FC} with $K = 3$ in the noisy reporting scenario.

decision thresholds at the RXs and FC for the OR rule, AND rule, and majority rule in Fig. 5(a), Fig. 5(b), and Fig. 5(c), respectively. The expected surfaces for the three fusion rules are obtained from (8)–(13) with (17) and (18). The values of ξ_{RX}° and ξ_{FC}°, associated with '■', for the OR rule, AND rule, and majority rule are obtained by solving (58), (59), and (60), respectively. The coordinates and values of '♦' and '■' in Figs. 5(a), 5(b), and 5(c) are summarized in Table III. Based on Table III, we quantify the accuracy loss caused by the suboptimal convex optimization for the OR rule, AND rule, and majority rule as 15.7%, 0%, and 14%, respectively. These small losses reveal that the joint ξ_{RX}° and ξ_{FC}° we find can achieve near-optimal error performance.

In Fig. 6, we consider a three-RX cooperative system and plot the average global error probability versus the radius of the FC for the AND rule, OR rule, and majority rule. The value of $\overline{Q}_{FC}^*$ for each r_{FC} in the expected curves for the three fusion rules are obtained via the exhaustive search of (8)–(13) with (17) and (18). The value of $\overline{Q}_{FC}$ for each r_{FC} in the approximated curves for the three fusion rules are obtained by first solving (58), (59), and (60), respectively, and then searching the actual values of $\overline{Q}_{FC}$ achieved by ξ_{RX}° and ξ_{FC}°. The simulation for approximated curves are obtained by considering ξ_{RX}° and ξ_{FC}° for each r_{FC}. We observe that for the AND rule and majority rule, the approximated curves well approximate the expected curves, which confirms the accuracy of jointly optimizing ξ_{RX}° and ξ_{FC}°. We also observe that for the OR rule, the approximated curve deviates from the expected curve when $r_{FC} = 0.225$ and $r_{FC} = 0.175$. This is due to

the fact that the global error probability is very sensitive to both thresholds in the region of ξ_{FC}^*. Furthermore, we observe that the approximated curves match the expected curves when $r_{FC} \leq 0.2\mu m$ for the AND rule, $r_{FC} \leq 0.15\mu m$ for the OR rule, and $r_{FC} \leq 0.175\mu m$ for the majority rule. Additionally, we observe that the expected error performance degrades as r_{FC} decreases for all the fusion rules. This can be explained by the fact that the reporting from the RXs to the FC becomes less reliable when r_{FC} decreases.

VI. CONCLUSIONS

In this paper, we optimized the error performance achieved by cooperative detection among distributed RXs in a diffusion-based MC system. For the perfect and noisy reporting scenarios, we derived closed-form expressions for the expected global error probability of the system having a symmetric topology. We also derived approximated expressions for the expected error probability in both reporting scenarios. We then found the convex constraints under which the approximated expressions are jointly convex with respect to the decision thresholds at the RXs and the FC. Based on the derived convex approximations and constraints, we formulated suboptimal convex optimization problems for the system in both reporting scenarios. Furthermore, we extended the suboptimal convex optimization problem for the instantaneous error performance to that for the average error performance over all transmitter symbol sequences. Using numerical and simulation results, we showed that the system error performance can be significantly improved by combining the detection information among distributed RXs, even when the total number of transmitted molecules is limited. We also showed that the suboptimal decision thresholds, obtained by solving our formulated convex optimization problems, achieve near-optimal global error performance. In our future work, we will explore the error performance analysis and optimization of soft fusion schemes at the fusion centre and the cooperative MC system with an asymmetric topology.

APPENDIX

PROOF OF THEOREM 3 AND THEOREM 4

The convexity of $\tilde{P}_{mdb}[j]^K$ can be proven by showing that its Hessian is positive semidefinite (PSD) [29]. Although the Hessian of $\tilde{P}_{mdb}[j]^K$ is not always PSD, we can show that the Hessian of $\tilde{P}_{mdb}[j]^K$ is PSD over a convex region if we impose a set of additional constraints. Recall that a matrix is PSD if and only if all of its principal minors are nonnegative [30]. Thus, we prove the joint convexity of $\tilde{P}_{mdb}[j]^K$ with respective to ξ_{RX} and ξ_{FC} by finding when $\frac{\partial^2 \tilde{P}_{mdb}[j]^K}{\partial \xi_{RX}^2} \geq 0$, $\frac{\partial^2 \tilde{P}_{mdb}[j]^K}{\partial \xi_{FC}^2} \geq 0$, and $\left(\frac{\partial^2 \tilde{P}_{mdb}[j]^K}{\partial \xi_{RX}^2} \right) \left(\frac{\partial^2 \tilde{P}_{mdb}[j]^K}{\partial \xi_{FC}^2} \right) - \left(\frac{\partial^2 \tilde{P}_{mdb}[j]^K}{\partial \xi_{RX} \xi_{FC}} \right)^2 \geq 0$.

We derive the second partial derivatives of $\tilde{P}_{mdb}[j]^K$ with respect to ξ_{RX} and ξ_{FC} as

$$\frac{\partial^2 \tilde{P}_{mdb}[j]^K}{\partial \xi_{RX}^2} = \Gamma\left(\xi_{RX}, \xi_{FC}, U_1[j], \overline{V}_1[j]\right)$$

$$= \left(-0.5 - U_1[j] + \xi_{RX}\right) \hat{\Upsilon}\left(K - 1, 1, 3/2\right)$$

$$+ (K - 1)\hat{\Upsilon}\left(K - 2, 2, 1\right) \tag{62}$$

and

$$\frac{\partial^2 \tilde{P}_{\mathrm{mdb}}[j]^K}{\partial \xi_{\mathrm{FC}}{}^2} = \Gamma\left(\xi_{\mathrm{FC}}, \xi_{\mathrm{RX}}, \overline{V}_1[j], U_1[j]\right), \qquad (63)$$

respectively, where

$$\hat{\Upsilon}\left(\alpha, \beta, \gamma\right) = \Bigg(\left(1 - \Lambda\left(\xi_{\mathrm{RX}}, U_1[j]\right)\right)\left(1 + \Lambda\left(\xi_{\mathrm{FC}}, \overline{V}_1[j]\right)\right)$$
$$+ 2\left(1 + \Lambda\left(\xi_{\mathrm{RX}}, U_1[j]\right)\right) \Bigg)^{\alpha}$$
$$\times \left(\Lambda\left(\xi_{\mathrm{FC}}, \overline{V}_1[j]\right) - 1\right)^{\beta} \frac{K\Theta\left(\xi_{\mathrm{RX}}, U_1[j]\right)^{\beta}}{U_1[j]^{\gamma} 4^{\alpha}\left(2\sqrt{2\pi}\right)^{\beta}}. \tag{64}$$

Since $\Lambda\left(x, \lambda\right)$ is between -1 and 1 and $\Theta\left(x, \lambda\right)$ is greater than zero, (62) and (63) are always nonnegative if we impose the convex constraints (22) and (50), respectively.

Finally, we show how the third condition of the joint convexity is satisfied. To this end, we derive the second mixed derivative of $\tilde{P}_{\mathrm{mdb}}[j]^K$ with respect to ξ_{RX} and ξ_{FC} as

$$\frac{\partial^2 \tilde{P}_{\mathrm{mdb}}[j]^K}{\partial \xi_{\mathrm{RX}} \xi_{\mathrm{FC}}} = \frac{2^{1-2K}K}{\pi\sqrt{U_1[j]\overline{V}_1[j]}} \Theta\left(\xi_{\mathrm{RX}}, U_1[j]\right)\Theta\left(\xi_{\mathrm{FC}}, \overline{V}_1[j]\right)$$
$$\times \Big(3 - \Lambda\left(\xi_{\mathrm{RX}}, U_1[j]\right)\left(1 + \Lambda\left(\xi_{\mathrm{FC}}, \overline{V}_1[j]\right)\right)$$
$$- \Lambda\left(\xi_{\mathrm{FC}}, \overline{V}_1[j]\right) \Big)^{-2+K}\Big(-4 + K$$
$$+ K\Lambda\left(\xi_{\mathrm{FC}}, \overline{V}_1[j]\right) + K\Lambda\left(\xi_{\mathrm{RX}}, U_1[j]\right)$$
$$\times \left(1 + \Lambda\left(\xi_{\mathrm{FC}}, \overline{V}_1[j]\right)\right) \Big). \tag{65}$$

Combining (62), (63), and (65), and performing some algebraic manipulations, we have

$$\left(\frac{\partial^2 \tilde{P}_{\mathrm{mdb}}[j]^K}{\partial \xi_{\mathrm{RX}}{}^2}\right)\left(\frac{\partial^2 \tilde{P}_{\mathrm{mdb}}[j]^K}{\partial \xi_{\mathrm{FC}}{}^2}\right) - \left(\frac{\partial^2 \tilde{P}_{\mathrm{mdb}}[j]^K}{\partial \xi_{\mathrm{RX}} \xi_{\mathrm{FC}}}\right)^2$$
$$= \Omega\left(\xi_{\mathrm{RX}}, \xi_{\mathrm{FC}}\right) \frac{K^2 2^{-4K}}{\pi^2 U_1[j]\overline{V}_1[j]} \Theta\left(\xi_{\mathrm{FC}}, \overline{V}_1[j]\right)\Theta\left(\xi_{\mathrm{RX}}, U_1[j]\right)$$
$$\times \Big(3 - \Lambda\left(\xi_{\mathrm{FC}}, \overline{V}_1[j]\right) - \Lambda\left(\xi_{\mathrm{RX}}, U_1[j]\right)$$
$$\times \left(1 + \Lambda\left(\xi_{\mathrm{FC}}, \overline{V}_1[j]\right)\right) \Big)^{\left(-4+2K\right)}, \tag{66}$$

where $\Omega\left(\xi_{\mathrm{RX}}, \xi_{\mathrm{FC}}\right)$ is shown in (67) at the top of page 16.

We note that (66) is always nonnegative if the following constraint is satisfied:

$$\Omega\left(\xi_{\mathrm{RX}}, \xi_{\mathrm{FC}}\right) \geq 0. \tag{68}$$

The constraint (68) is not convex, and ξ_{RX} and ξ_{FC} in the exponential and error functions make joint convexity analysis with respect to ξ_{RX} and ξ_{FC} cumbersome. To tackle this cumbersomeness, we can bound ξ_{RX} with ξ_{RX}^- or ξ_{RX}^+, and bound ξ_{FC} with ξ_{FC}^- or ξ_{FC}^+ to lower the value of the left-hand side of (68). Thus, we obtain (51) to ensure that (66) is always nonnegative. Under the constraints (22), (50), and (51), we define a convex region where $\tilde{P}_{\mathrm{mdb}}[j]^K$ is jointly convex with respect to ξ_{FC} and ξ_{RX}.

Similar to the proof of the joint convexity of $\tilde{P}_{\mathrm{mdb}}[j]^K$, it can be proven that $\tilde{P}_{\mathrm{fab}}[j]^K$ is also jointly convex with respect to ξ_{RX} and ξ_{FC} under the constraints (23), (53), and (54).

REFERENCES

[1] Y. Fang, A. Noel, N. Yang, A. W. Eckford, and R. A. Kennedy, "Distributed cooperative detection for multi-receiver molecular communication," in Proc. *IEEE GLOBECOM 2016*, Washington, DC, Dec. 2016.

[2] I. F. Akyildiz, F. Brunetti, and C. Blazquez, "Nanonetworks: A new communication paradigm," *Comput. Networks*, vol. 52, no. 12, pp. 2260-2279, May 2008.

[3] T. Nakano, M. J. Moore, F. Wei, A. V. Vasilakos, and J. Shuai, "Molecular communication and networking: Opportunities and challenges," *IEEE Trans. NanoBiosci.*, vol. 11, no. 2, pp. 135-148, June 2012.

[4] T. Nakano, A. W. Eckford, and T. Haraguchi, *Molecular Communication*. Cambridge, UK: Cambridge University Press, 2013.

[5] N. Farsad, H. B. Yilmaz, A. Eckford, C.-B. Chae, and W. Guo, "A comprehensive survey of recent advancements in molecular communication," *IEEE Commun. Surveys & Tutorials*, vol. 18, no. 3, pp. 1887–1919, Aug. 2016.

[6] B. Atakan and O. B. Akan, "Single and multiple-access channel capacity in molecular nanonewtorks," in *Proc. ICST Nano-Net 2009*, Luzern, Switzerland, Mar. 2009, pp. 14–23.

[7] M. T. Barros, S. Balasubramaniam, and B. Jennings, "Comparative end-to-end analysis of Ca^{2+}-signaling-based molecular communication in biological tissues," *IEEE Trans. Commun.*, vol. 63, no. 12, pp. 5128–5142, Dec. 2015.

[8] S. M. Baylor and S. Hollingworth, "Calcium indicators and calcium signalling in skeletal muscle fibres during excitation-contraction coupling," *Prog. Biophys. Mol. Biol.*, vol. 105, pp. 162–179, June 2010.

[9] B. Atakan and O. B. Akan, "On molecular multiple-access, broadcast, and relay channels in nanonetworks," in *Proc. ICST BIONETICS 2008*, Hyogo, Japan, Nov. 2008, pp. 16:1–16:8.

[10] M. J. Moore, T. Suda, and K. Oiwa, "Molecular communication: Modeling noise effects on information rate," *IEEE Trans. NanoBiosci.*, vol. 8, no. 2, pp. 169–179, June 2009.

[11] Y. Okaie, T. Obuchi, T. Hara, and S. Nishio, "In silico experiments of mobile bionanosensor networks for target tracking," in *Proc. ACM NANOCOM 2015*, Boston, MA, Sept. 2015, pp. 14:1–14:6.

[12] A. Einolghozati, M. Sardari, and F. Fekri, "Design and analysis of wireless communication systems using diffusion-based molecular communication among bacteria," *IEEE Trans. Wireless Commun.*, vol. 12, no. 12, pp. 6096–6105, Dec. 2013.

[13] A. O. Bicen and I. F. Akyildiz, "Interference modeling and capacity analysis for microfluidic molecular communication channels," *IEEE Trans. Nanotechnol.*, vol. 14, no. 13, pp. 570–579, May 2015.

[14] T. Nakano, Y. Okaie, and A. V. Vasilakos, "Transmission rate control for molecular communication among biological nanomachines," *IEEE J. Sel. Areas Commun.*, vol. 31, no. 12, pp. 835–846, Dec. 2013.

[15] C. T. Chou, "Extended master equation models for molecular communication networks," *IEEE Trans. NanoBiosci.*, vol. 12, no. 2, pp. 79–92, June 2013.

[16] B. H. Koo, C. Lee, H. B. Yilmaz, N. Farsad, A. Eckford, and C. B. Chae, "Molecular MIMO: From theory to prototype," *IEEE J. Sel. Areas Commun.*, vol. 34, no. 3, pp. 600–614, Mar. 2016.

[17] l. Akyildiz, B. Lo, and R. Balakrishnan, "Cooperative spectrum sensing in cognitive radio networks: A survey," *Phys. Commun.*, vol. 4, no. 1, pp. 40–62, Mar. 2011.

[18] P. K. Varshney, *Distributed Detection and Data Fusion*. New York, NY: Springer-Verlag, 1997.

[19] A. P. de Silva and S. Uchiyama, "Molecular logic and computing," *Nature Nanotech.*, vol. 2, no. 7, pp. 399–410, July 2007.

[20] U. Pischel, "Chemical approaches to molecular logic elements for addition and subtraction," *Angew. Chem. Int. Ed.*, vol. 46, no. 22, pp. 4026–4040, 2007.

[21] J. N. Laneman, D. N. C. Tse, and G. W. Wornell, "Cooperative diversity in wireless networks: Efficient protocols and outage behavior," *IEEE Trans. Inf. Theory*, vol. 50, no. 12, pp. 3062–3080, Nov. 2004.

[22] A. Ahmadzadeh, A. Noel, and R. Schober, "Analysis and design of multi-hop diffusion-based molecular communication networks," *IEEE Trans. Mol. Biol. Multi-Scale Commun.*, vol. 1, no. 2, pp. 144–157, June 2015.

[23] S. Ross, *Introduction to Probability and Statistics for Engineers and Scientists*, 4th ed. New York: Academic, 2009.

[24] M. S. Kuran, H. B. Yilmaz, T. Tugcu and I. F. Akyildiz, "Modulation techniques for communication via diffusion in nanonetworks," in *Proc. IEEE ICC 2011*, Kyoto, Japan, June 2011, pp. 1-5.

$$\Omega\left(\xi_{\text{RX}}, \xi_{\text{FC}}\right) = -4\Theta\left(\xi_{\text{RX}}, U_1[j]\right)\left(-4 + K + K\Lambda\left(\xi_{\text{FC}}, \overline{V}_1[j]\right) + K\Lambda\left(\xi_{\text{RX}}, U_1[j]\right)\left(1 + \Lambda\left(\xi_{\text{FC}}, \overline{V}_1[j]\right)\right)\right)^2 + \frac{\left(1 + \Lambda\left(\xi_{\text{RX}}, U_1[j]\right)\right)}{\sqrt{U_1[j]\overline{V}_1[j]}}$$

$$\times \left(1 + \Lambda\left(\xi_{\text{FC}}, \overline{V}_1[j]\right)\right)\left(2\left(-1 + K\right)\sqrt{\overline{V}_1[j]}\left(1 + \Lambda\left(\xi_{\text{RX}}, U_1[j]\right)\right) - \frac{\sqrt{2\pi}}{\Theta\left(\xi_{\text{FC}}, \overline{V}_1[j]\right)}\left(0.5 + \overline{V}_1[j] - \xi_{\text{FC}}\right)\right.$$

$$\times \left(-3 + \Lambda\left(\xi_{\text{FC}}, \overline{V}_1[j]\right) + \Lambda\left(\xi_{\text{RX}}, U_1[j]\right)\left(1 + \Lambda\left(\xi_{\text{FC}}, \overline{V}_1[j]\right)\right)\right)\right)\left(\Theta\left(\xi_{\text{RX}}, U_1[j]\right)\left(-1 + K\right)\left(1 + \Lambda\left(\xi_{\text{FC}}, \overline{V}_1[j]\right)\right)\right.$$

$$\times 2\sqrt{U_1[j]} - \sqrt{2\pi}\left(0.5 + U_1[j] - \xi_{\text{RX}}\right)\left(-3 + \Lambda\left(\xi_{\text{FC}}, \overline{V}_1[j]\right) + \Lambda\left(\xi_{\text{RX}}, U_1[j]\right)\left(1 + \Lambda\left(\xi_{\text{FC}}, \overline{V}_1[j]\right)\right)\right)\right) \tag{67}$$

[25] A. Noel, K. C. Cheung, and R. Schober, "Optimal receiver design for diffusive molecular communication with flow and additive noise," *IEEE Trans. NanoBiosci.*, vol. 13, no. 3, pp. 350–362, Sept. 2014.

[26] H. ShahMohammadian, G. G. Messier, and S. Magierowski, "Blind synchronization in diffusion-based molecular communication channels," *IEEE Commun. Lett.*, vol. 17, no. 11, pp. 2156–2159, Nov. 2013.

[27] S. Abadal and I. F. Akyildiz, "Bio-inspired synchronization for nanocommunication networks," in *Proc. IEEE GLOBECOM*, Dec. 2011, pp. 1–5.

[28] A. Noel, K. C. Cheung, and R. Schober, "Using dimensional analysis to assess scalability and accuracy in molecular communication," in *Proc. IEEE ICC 2013 MoNaCOM Workshop*, Budapest, Hungary, June 2013, pp. 818–823.

[29] S. Boyd and L. Vandenberghe, *Convex Optimization*. Cambridge University Press, 2004.

[30] R. Horn and C. Johnson, *Matrix Analysis*. Cambridge University Press, 1985.

[31] Y. Fang, A. Noel, N. Yang, A. W. Eckford, and R. A. Kennedy, "Convex optimization of distributed cooperative detection in multi-receiver molecular communication," submitted to *IEEE Trans. Mol. Bio. Multi-Scale Commun.*, 2016. [Online]. Available: arXiv:1611.05590